Stem Cell Reports
Article

ISSCR

OPEN ACCESS

CABLES1 Deficiency Impairs Quiescence and Stress Responses of Hematopoietic Stem Cells in Intrinsic and Extrinsic Manners

Liang He,[1,2,3,4] Florian Beghi,[1,2,3] Viviane Baral,[1,2,3] Mallorie Dépond,[1,2,3] Yanyan Zhang,[1,2,3] Virginie Joulin,[1,2,3] Bo R. Rueda,[5] Patrick Gonin,[6] Adlen Foudi,[7] Monika Wittner,[1,2,3,8,9] and Fawzia Louache[1,2,3,8,9,*]

[1]Institut National de la Santé et de la Recherche Médicale, Inserm UMRS1170, 114 Rue Edouard Vaillant, 94805 Villejuif, France
[2]Paris-Saclay University, Villejuif, France
[3]Gustave Roussy, 114 Rue Edouard Vaillant, 94805 Villejuif, France
[4]Department of Obstetrics and Gynecology, Tongji Hospital, Tongji Medical College, Huazhong University of Science and Technology, Wuhan, P.R. China
[5]Vincent Center for Reproductive Biology, Department of Obstetrics and Gynecology, Massachusetts General Hospital, Boston, USA
[6]Plateforme d'Evaluation Préclinique, AMMICA UMS 3655/ US 23, Gustave Roussy, Villejuif, France
[7]Paris-Saclay University, UFR Medicine, INSERM UMS 33, Andre Lwoff Institute, Paul Brousse Hospital, Villejuif, France
[8]CNRS, GDR 3697 MicroNiT, Tours, France
[9]Co-senior author
*Correspondence: fawzia.louache@gustaveroussy.fr
https://doi.org/10.1016/j.stemcr.2019.06.002

SUMMARY

Bone marrow (BM) niche cells help to keep adult hematopoietic stem cells (HSCs) in a quiescent state via secreted factors and induction of cell-cycle inhibitors. Here, we demonstrate that the adapter protein CABLES1 is a key regulator of long-term hematopoietic homeostasis during stress and aging. Young mice lacking *Cables1* displayed hyperproliferation of hematopoietic progenitor cells. This defect was cell intrinsic, since it was reproduced in BM transplantation assays using wild-type animals as recipients. Overexpression and short hairpin RNA-mediated depletion of CABLES1 protein resulted in $p21^{Cip/waf}$ up- and downregulation, respectively. Aged mice lacking *Cables1* displayed abnormalities in peripheral blood cell counts accompanied by a significant reduction in HSC compartment, concomitant with an increased mobilization of progenitor cells. In addition, *Cables1*$^{-/-}$ mice displayed increased sensitivity to the chemotherapeutic agent 5-fluorouracil due to an abnormal microenvironment. Altogether, our findings uncover a key role for CABLES1 in HSC homeostasis and stress hematopoiesis.

INTRODUCTION

Maintenance of the hematopoietic system requires continuous cellular replenishment from a rare population of hematopoietic stem cells (HSCs) endowed with self-renewal and multilineage differentiation capacities (Orkin and Zon, 2008). At steady state, in the bone marrow (BM) the majority of HSCs remain quiescent in the G_0 phase of the cell cycle (Bernitz et al., 2016; Foudi et al., 2009). When stress occurs and the number of mature cells is reduced in the blood circulation (e.g., bleeding, infection, or chemical/radiation injury), HSCs rapidly enter the cell cycle to give rise to progenitor cells with robust proliferative potential, allowing replenishment of the hematopoietic system (Pietras et al., 2014). However, when HSCs are submitted to frequent proliferative stress situations, self-renewal is severely impeded. Similarly, HSCs accumulate changes with age that include a decrease in the regenerative potential and a preferential differentiation into myeloid cells with a loss of support of B cell lineage. Although aging of HSCs was initially thought to be solely influenced by stem cell-intrinsic mechanisms, several recent data indicate that aging of the niche and the microenvironment contribute to aging-associated phenotypes of HSCs (Florian et al., 2012; Rossi et al., 2005).

The cyclin-dependent kinase (Cdk) 5 and Abl enzyme substrate 1 (CABLES1), also called Ik3-1, is a Cdk-interacting protein that binds to multiple Cdks including Cdk2 (Wu et al., 2001), Cdk3 (Yamochi et al., 2001), and Cdk5 (Zukerberg et al., 2000). Probably due to its potential to interaction with Cdk, CABLES1 inhibits proliferation in cell line models by enhancing the inhibitory function of Cdk2 mediated by Wee1 (Wu et al., 2001). It also regulates cell proliferation by stabilizing $p21^{Cip/waf}$ (p21) (Shi et al., 2014). In addition to an impact on proliferation, CABLES1 can induce cell death by regulating stability and proteasomal degradation of several members of the p53 family including p53, p73, and TAp63a (Matsuoka et al., 2003; Tsuji et al., 2002). In addition, CABLES1 links Robo-bound Abl kinase to N-cadherin, regulating β-catenin function and transcription (Rhee et al., 2007). Likely due in part to its ability to negatively regulate proliferation and induce apoptosis, loss of CABLES1 is associated with a high frequency in multiple types of cancer in humans, including endometrial cancer (DeBernardo et al., 2005), colorectal cancer (Park et al., 2007), ovarian cancer (Dong et al., 2003), and non-small cell lung cancer (Huang et al., 2017). In mouse models, loss of *Cables1* results in a high incidence of endometrial adenocarcinoma (Zukerberg et al., 2004). In addition, *Cables1* acts as tumor suppressor,

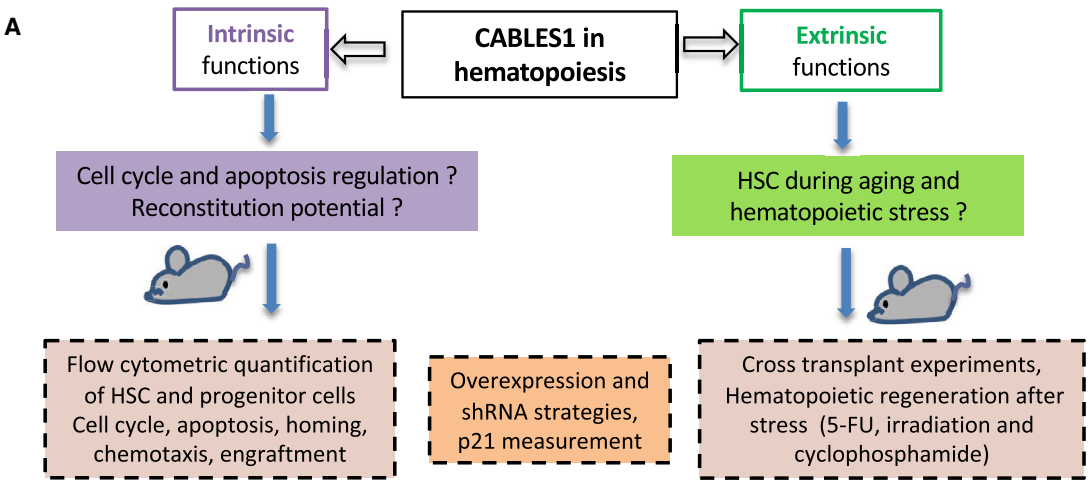

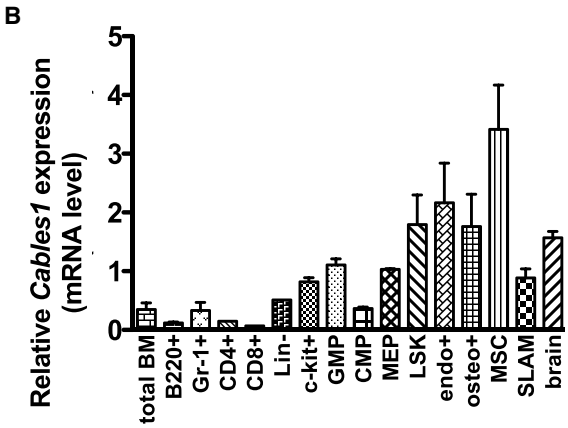

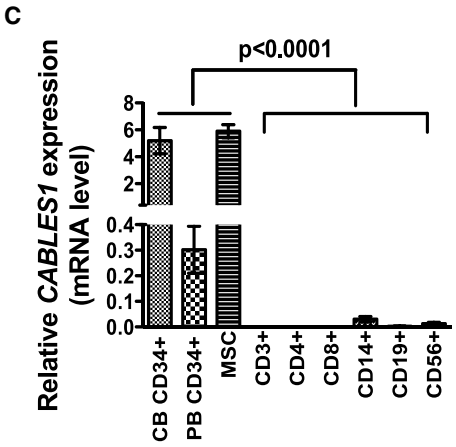

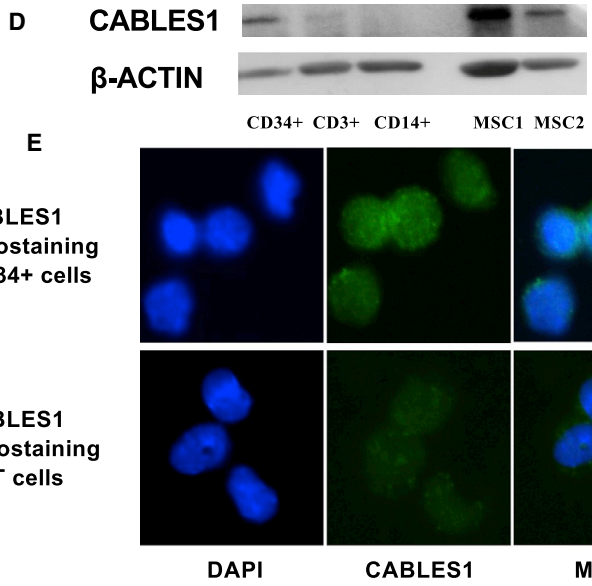

(legend on next page)

regulating intestinal tumor progression in Apc^{Min} mice (Arnason et al., 2013). Despite its well-recognized role in cancer, only a few studies have addressed its function in physiologic settings. Current studies indicate a role of CABLES1 in neural differentiation and neurite outgrowth by interacting with Cdk5 (a non-cell-cycle-associated kinase) and Abl (Zukerberg et al., 2000). Moreover, CABLES1 is required for embryonic neural development in the zebrafish model (Groeneweg et al., 2011). Finally, loss of CABLES1 enhances oogenesis associated with reduced oocyte quality (Lee et al., 2007).

Previous studies reported that loss of *Cables1* results in an increase of BM hematopoietic progenitor cells, suggesting that CABLES1 could be a potent regulator of hematopoiesis (Lee et al., 2007). Here, we broaden our understanding of CABLES1 function(s) in hematopoiesis using a $Cables1^{-/-}$ mouse model. We first report that CABLES1 is predominantly expressed in the progenitor cell compartment, suggesting that CABLES1 is a stemness marker. We also show that absence of *Cables1* in mice markedly affects progenitor cell proliferation. Under stress conditions, absence of *Cables1* delays hematopoietic recovery, while during aging the HSC number is impaired. Finally, the number of mesenchymal stromal cells is reduced in $Cables1^{-/-}$ mice. Thus, CABLES1 participates in the control of HSC maintenance during aging and under hematopoietic stress.

RESULTS

CABLES1 Is Expressed in Hematopoietic Stem and Progenitor Cells and in Niche Cells

The experimental strategy to analyze CABLES1 function in hematopoiesis is depicted in Figure 1A. The mRNA expression levels of *Cables1* in cells of the hematopoietic and BM microenvironment lineages were analyzed by qRT-PCR. We isolated different subsets of primitive hematopoietic progenitor cells (Kiel et al., 2005; Morita et al., 2010) and used the mouse brain as reference, as previously described (Zukerberg et al., 2000). *Cables1* mRNA expression level was substantially higher in LSK ($Lin^-Kit^+Sca\text{-}1^+$) cells and SLAM ($CD150^+CD48^-$ LSK) cells compared with differentiated cells, such as $B220^+$, $CD4^+$, $CD8^+$, and $Gr\text{-}1^+$ cells (Figure 1B). We also performed analysis of *Cables1* expression in BM niche cells such as osteoblasts, endothelial cells, and mesenchymal stem cells (MSCs) (Mendez-Ferrer et al., 2015). All three sorted cell populations expressed *Cables1* mRNAs (Figure 1B). Of note, the expression of *Cables1* mRNA was not modified during aging in mice (Figure S1). *CABLES1* was also expressed in human $CD34^+$ progenitor cells from cord blood (CB-$CD34^+$), mobilized peripheral blood (PB-$CD34^+$) and human MSCs, in contrast to mature cell populations (Figure 1C). These results were confirmed at the protein level (Figures 1D, S2A, and S2B). In addition, the localization of CABLES1 protein in CB-$CD34^+$ cells was mainly nuclear (Figure 1E). These findings suggest that CABLES1 is expressed in the adult BM.

Steady-State Hematopoiesis in Young Mice Is Not Affected by Cables1 Deficiency

To address the impact of loss of *Cables1* in hematopoiesis, we assessed complete blood counts in $Cables1^{-/-}$ and wild-type (WT) mice. Numbers of white blood cells (WBCs), red blood cells (RBCs) and platelets (PLTs) were within normal ranges in 10- to 12-week-old animals (Figures S3A–S3C) as well as the percentages of B lymphocytes, T lymphocytes, and neutrophils (Figure S3D). BM and spleen cellularities were also comparable between $Cables1^{-/-}$ mice and their normal counterparts (Figures S4A and S4B). No significant differences in the number of colony-forming unit cells (CFU-Cs) (Figure S4C) and phenotypically defined progenitor cells including granulomonocytic progenitors (GMPs), common myeloid progenitors (CMPs), common lymphoid progenitors (CLPs), and mega-erythroid progenitors (MEPs) were noted between $Cables1^{-/-}$ and WT mice

Figure 1. CABLES1 Expression in Human and Murine Hematopoietic and Niche Cells

(A) Experimental strategy used to probe functions of CABLES1 in hematopoiesis. HSC, hematopoietic stem cells; shRNA, short hairpin RNA; 5-FU, 5-fluorouracil.

(B) *Cables1* mRNA expression in mouse cells sorted by fluorescence-activated cell sorting: B cells ($B220^+$), T cells ($CD4^+$ and $CD8^+$), myeloid ($Gr\text{-}1^+$) cells, Lin^- (lineage marker-negative cells, namely $CD3^-B220^-Ter119^-Gr\text{-}1^-$), LSK ($Lin^-c\text{-}Kit^+Sca\text{-}1^+$), c-kit$^+$ ($Lin^-c\text{-}Kit^+Sca\text{-}1^-$), SLAM ($CD150^+CD48^-$LSK), CMPs ($Lin^-Sca\text{-}1^+c\text{-}Kit^+FcR^-CD34^+$), GMP ($Lin^-Sca\text{-}1^+c\text{-}Kit^+FcR^+CD34^+$), MEP ($Lin^-Sca\text{-}1^+c\text{-}Kit^+FcR^-CD34^-$); and in cellular components of the BM microenvironment: osteoblasts ($CD45^-Ter119^-CD31^-Sca\text{-}1^-CD51^+$), endothelial cells ($CD45^-Ter119^-CD31^+$), and MSCs ($CD45^-Ter119^-CD31^-Sca^+CD51^+$). Data are normalized to HPRT transcript levels and mouse brain is used as reference. Data represent a pool from 10 mice and are the mean ± SEM of triplicates. See also Figure S1.

(C) CABLES1 expression in human $CD34^+$ cells from cord blood (CB-$CD34^+$), mobilized peripheral blood (PB-CD34), and mature blood cells ($CD4^+$, $CD8^+$, $CD14^+$, $CD19^+$, $CD56^+$). Data are normalized to HPRT transcript levels and $CD34^+$ cells are used as reference.

(D) Expression level of human CABLES1 in CB-$CD34^+$, $CD3^+$, $CD14^+$, and MSCs by western blot. Two different MSC samples are shown as MSC1 and MSC2. See also Figure S2.

(E) Immunolocalization of CABLES1 in CB-$CD34^+$ cells. Staining with the anti-CABLES1 antibody of human $CD3^+$ cells that do not express significant levels of *CABLES1* mRNA is presented in the lower panel.

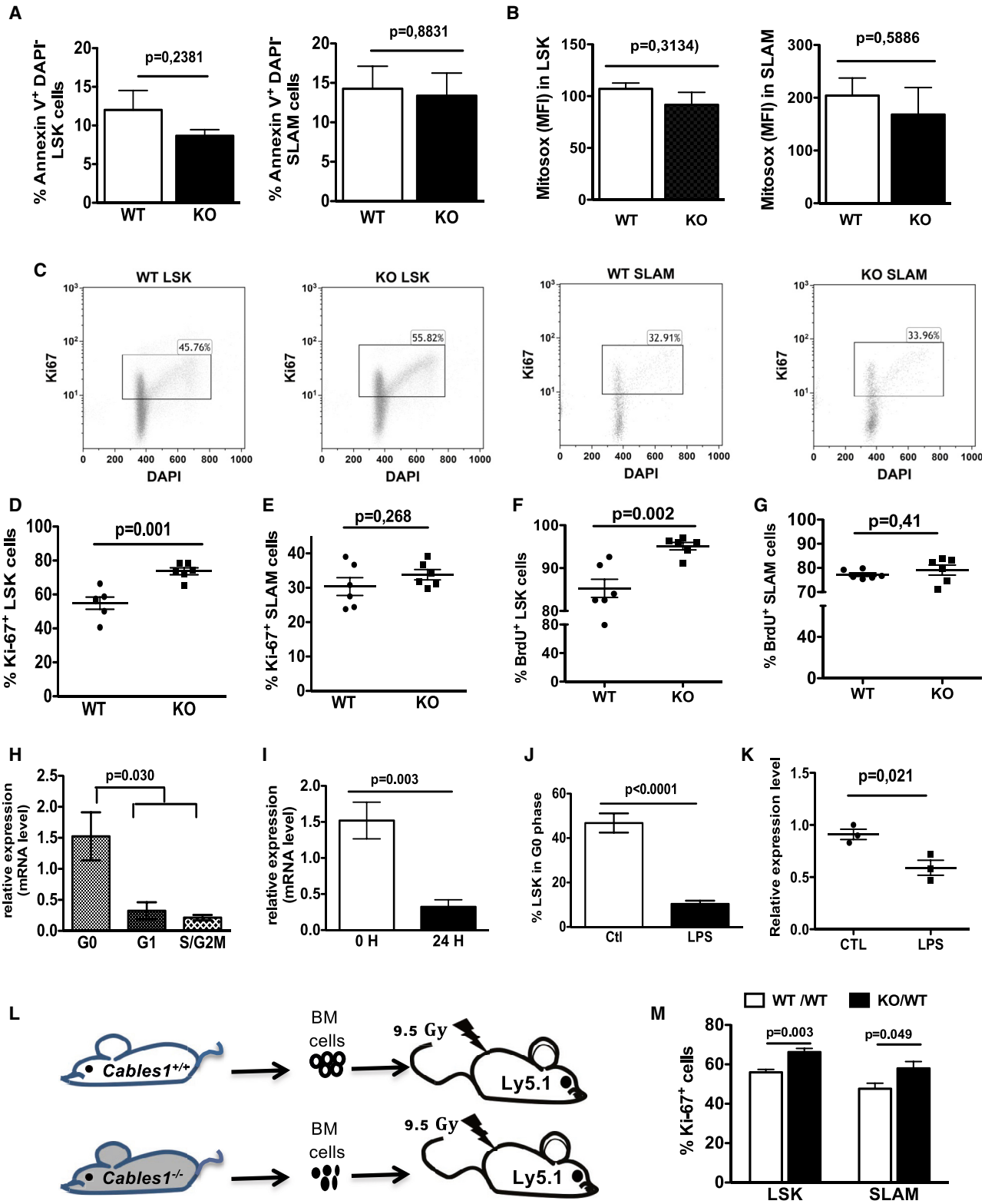

(legend on next page)

(Figures S4D and S4E). Finally, the numbers of phenotypically defined LT-HSC ($CD150^+CD48^-KSL$) were similar between the two groups (Figure S4F). These data demonstrate that loss of *Cables1* does not have a major impact on steady-state hematopoiesis and suggest that blood production is not affected by *Cables1* deficiency.

Cables1 Is an Intrinsic Cell-Cycle Inhibitor in Mouse Progenitor Cells

As CABLES1 is highly expressed in hematopoietic progenitor cells and is involved in cell-cycle regulation and cell death as shown in previous *in vitro* studies (Huang et al., 2017), we evaluated its impact on apoptosis, the levels of mitochondrial reactive oxygen species (ROS), and cell-cycle status of hematopoietic progenitor cells under steady-state conditions. In 10- to 12-week-old *Cables1*$^{-/-}$ mice, the proportions of annexin V^+ $DAPI^-$ LSK and SLAM cells and mitochondrial ROS levels were not altered compared with *Cables1*$^{+/+}$ mice (Figures 2A and 2B). However, as illustrated in Figure 2C, the fraction of cycling cells ($Ki67^+$) among LSK cells was significantly higher in the BM of *Cables1*$^{-/-}$ mice compared with WT mice (Figure 2D). Of note, within the more immature subset of HSCs, namely the SLAM population, the proportion of $Ki67^+$ cells was not affected (Figure 2E). To confirm these results, we performed *in vivo* bromodeoxyuridine (BrdU) incorporation assays. In accordance with the Ki67 assays, a higher number of *Cables1*$^{-/-}$ LSK cells were BrdU positive (Figure 2F), whereas the proportion of $BrdU^+$ cells in the SLAM cell population was not altered (Figure 2G). As CABLES1 is a cell-cycle inhibitor for LSK progenitor cells, we compared its expression between G_0 and cycling LSK cells. We sorted LSK cells in the G_0, G_1, and $S/G_2/M$ phase using Pyronin Y and Hoechst 33342 staining and tested the relative expression of *Cables1* by qPCR. LSK cells in the G_0 phase showed the highest expression level of *Cables1* compared with LSK cells in the G_1 and $S/G_2/M$ phase (Figure 2H). In addition, *Cables1* expression sharply decreased upon culture of freshly isolated LSK cells in cytokine-containing medium (Figure 2I). Similarly, *in vivo* treatment of mice with lipopolysaccharide (LPS), leading to quiescence loss of hematopoietic progenitor cells (Figure 2J), was associated with a sharp decrease in *Cables1* expression (Figure 2K). Altogether, these results suggest that *CABLES1* expression negatively regulates the cell-cycle status of hematopoietic progenitor cells.

As cells from the hematopoietic microenvironment also express CABLES1, we sought to discover whether the role of CABLES1 in progenitor cell proliferation was intrinsic or extrinsic. Thus, we conducted transplantation assays using donor BM cells from *Cables1*$^{-/-}$ or *Cables1*$^{+/+}$ (Ly5.2) mice that were transplanted into lethally irradiated recipient mice (Ly5.1) (Figure 2L). Three months after transplantation, the donor contribution was over 90% for each group (Figures S3E and S3F–S3H). *Cables1*-null derived LSK and SLAM cells had significantly higher proportions of Ki67-proliferating cells than their WT counterparts (Figure 2M). This illustrates the intrinsic role of CABLES1 in regulating the proliferative status of hematopoietic progenitor cells.

Cables1$^{-/-}$ HSCs Harbor Higher Reconstitution Fitness

We next evaluated the impact of *Cables1* deficiency in competitive transplantation. BM cells from *Cables1*$^{-/-}$ (Ly5.2) or *Cables1*$^{+/+}$ (Ly5.2) mice were mixed 1:1 with age-matched BM competitor cells (Ly5.1) and injected into lethally irradiated recipient mice (Ly5.1) (Figure 3A). During 5 continuous months after transplantation,

Figure 2. CABLES1 Is an Intrinsic Cell-Cycle Inhibitor in HSCs of Young Mice

(A) Frequencies of annexin V^+ cells in BM LSK and SLAM populations.

(B) Mitosox staining in BM LSK and SLAM cells of 12-week-old WT and *Cables1*$^{-/-}$ mice. Data are mean ± SEM from six mice per group, pooled from two independent experiments.

(C) Representative flow-cytometric images of cell-cycle analysis by Ki67/DAPI costaining.

(D and E) Frequencies of $Ki67^+$ cells in BM LSK and SLAM cells.

(F and G) Frequencies of $BrdU^+$ cells in LSK and SLAM cells. In (A) to (G), five mice were analyzed for each genotype and data represent mean ± SEM.

(H) *Cables1* mRNA expression in LSK cells in the G_0, G_1, or $S/G_2/M$ phase. Data represent a pool of 10 mice and mean ± SEM of three independent experiments.

(I) *Cables1*$^{-/-}$ mRNA expression in LSK cells cultured in cytokine-containing medium (mouse stem cell factor, IL3, Flt3L) for 24 h; 0 H represents isolated LSK cells before culture. Data are mean ± SEM of three independent experiments.

(J) Frequencies of LSK cells in the G_0 phase ($Ki67^-/DAPI^-$) 24 h after treatment of mice with LPS (n = 6).

(K) *Cables1*$^{-/-}$ mRNA expression in LSK cells from LPS-treated mice.

(L) Schematic representation of transplantation: *Cables1*$^{-/-}$ or WT BM donor cells were transplanted into lethally irradiated Ly5.1 mice (n = 5).

(M) Frequencies of $Ki67^+$ LSK and SLAM cells 3 months after reconstitution (see also Figures S3E–S3H). qPCRs are normalized to expression of HPRT. Data are mean ± SEM; unpaired Student's two-tailed t test was performed for statistical analysis. LPS, lipopolysaccharides.

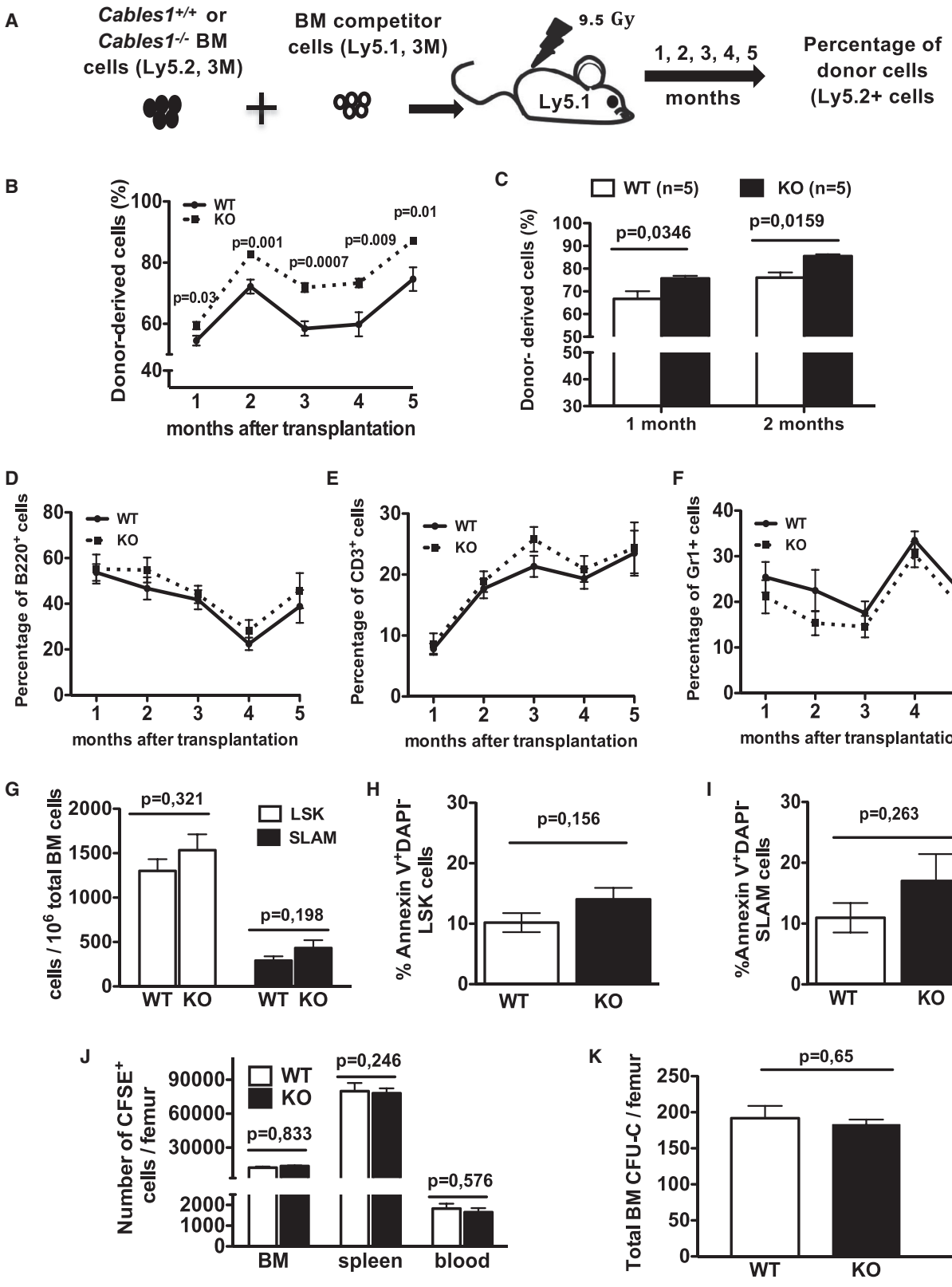

(legend on next page)

recipients were analyzed monthly for the percentage of Ly5.2 donor-derived cells in blood. There was significantly 5%, 10%, 13.4%, 13%, and 13% more *Cables1*$^{-/-}$-derived cells in the blood of Ly5.1 recipients at 1, 2, 3, 4, and 5 months post reconstitution, respectively (Figure 3B). A similar higher reconstitution level was observed when *Cables1*$^{-/-}$ LSK cells were transplanted (Figure 3C). The percentages of Ly5.2 donor-derived B cells (Figure 3D), T cells (Figure 3E), and granulocytes (Figure 3F) were similar between the two groups.

The frequency of *Cables1*$^{-/-}$ BM LSK and SLAM cells tended to be higher than that of *Cables1*$^{+/+}$ LSK and SLAM cells in transplanted animals, but this was not significant (Figure 3G). To characterize the enhanced competitive properties of *Cables1*$^{-/-}$ HSCs, we measured the apoptotic rate of LSK and SLAM cells after transplantation. LSK and SLAM cells from *Cables1*$^{-/-}$ mice had similar apoptotic rates compared with *Cables1*$^{+/+}$ LSK and SLAM cells (Figures 3H and 3I). We also conducted homing experiments. Carboxyfluorescein succinimidyl ester (CFSE)-marked *Cables1*$^{-/-}$ or *Cables1*$^{+/+}$ BM cells were injected into irradiated recipient mice. The numbers of CFSE^{+} *Cables1*$^{-/-}$ or *Cables1*$^{+/+}$ cells in the BM, spleen, and blood of recipients were comparable (Figure 3J). The number of progenitor cells that homed to the BM was similar between *Cables1*$^{-/-}$ or *Cables1*$^{+/+}$ genotypes (Figure 3K). Thus, the enhanced competitive capacity of *Cables1*$^{-/-}$ HSC is due to neither increased homing capacity nor decreased apoptosis and could be related to their enhanced cell-cycle entry under transplantation settings.

CABLES1 Slows Cell Proliferation of Human CD34^{+} Cells and Regulates p21 Level

To examine whether CABLES1 could regulate the proliferation of human hematopoietic progenitor cells, we transduced CB CD34^{+} cells using lentiviral vectors encoding either GFP alone or human CABLES1 (Figure S5A). Transduced cells were sorted based on GFP expression (Figure S5B) and CABLES1 overexpression was verified by western blotting (Figure 4A). GFP^{+} cells were seeded in methylcellulose to assess the effect of CABLES1 on proliferation of hematopoietic progenitor cells. CABLES1 overexpression not only reduced the number of colonies but also diminished their size (Figures 4B and 4C). Thus, CABLES1 could slow the proliferation of hematopoietic progenitor cells.

To further investigate the effect of CABLES1 on cell proliferation, we next silenced *CABLES1* expression in CB-CD34^{+} cells using a short hairpin RNA (shRNA) strategy. A sharp reduction of *CABLES1* mRNA was observed using two different shRNAs (Figures 4D and S5C), and decreased protein levels (Figure 4E) were confirmed in *CABLES1* shRNA-transduced CD34^{+} cells compared with control shRNA-transduced CD34^{+} cells. The proliferation rate of CD34^{+} cells transduced with *CABLES1* shRNA was higher compared with control shRNA-transduced cells (Figure 4F). CABLES1 has previously been demonstrated to interact with the master regulator CDKI p21, inducing inhibition of cell proliferation and apoptosis (Shi et al., 2014). Thus, we investigated the potential role of p21 in CABLES1 effects on cell proliferation. Similarly to murine progenitor cells, CABLES1 expression decreased upon cytokine stimulation of CD34^{+} cells (Figure 4G). This decrease was accompanied by a parallel reduction in the level of p21 protein expression (Figure 4H). Strikingly, an increase in p21 protein expression was found in CB-CD34^{+} cells overexpressing CABLES1 compared with control GFP-expressing cells (Figure 4I). Furthermore, a reduction in p21 protein level was observed in *CABLES1* shRNA-transduced CD34^{+} cells compared with control shRNA-transduced CD34^{+} cells (Figure 4J). No change in p21 mRNA expression was noted in *CABLES1* shRNA-transduced CD34^{+} cells compared with control shRNA-transduced CD34^{+} cells (data not shown). To assess whether our *in vitro* results on human cells were representative of the CABLES1-p21 link, we evaluated p21 protein level in murine *Cables1* WT and knockout (KO) LSK and SLAM cells. In accordance with our *in vitro* strategy using shRNA in human cells, our analysis showed that the protein levels of p21 was decreased in *Cables1*$^{-/-}$ LSK (Figure 4K) and LSK SLAM cells (Figure 4L). Thus, our results suggest a role for CABLES1 in the regulation of p21 protein expression.

Figure 3. Cables1$^{-/-}$ HSCs Harbor Higher Reconstitution Fitness

(A) Schematic representation of competitive repopulation assays.

(B) Contributions of donor cells (CD45.2^{+}) in blood of recipient mice after transplantation of unfractionated BM cells.

(C) Contributions of donor cells (CD45.2^{+}) in blood of recipient mice after transplantation of purified BM LSK cells.

(D–F) Frequencies of (D) donor-derived B cells, (E) T cells, and (F) granulocytes.

(G) Frequencies of donor-derived CD45.2^{+} LSK and SLAM cells in recipients' BM 2 months after reconstitution (n = 5 per group).

(H and I) Percentages of (H) apoptotic donor-derived LSK and (I) SLAM cells.

(J) Numbers of CFSE-labeled *Cables1*$^{-/-}$ or WT BM cells, evaluated 16 h after homing to BM and spleen of lethally irradiated recipients (n = 6).

(K) CFU-C numbers per femur in the BM 4 h after injection.

All values are mean ± SEM; unpaired Student's two-tailed t test was performed for statistical analysis.

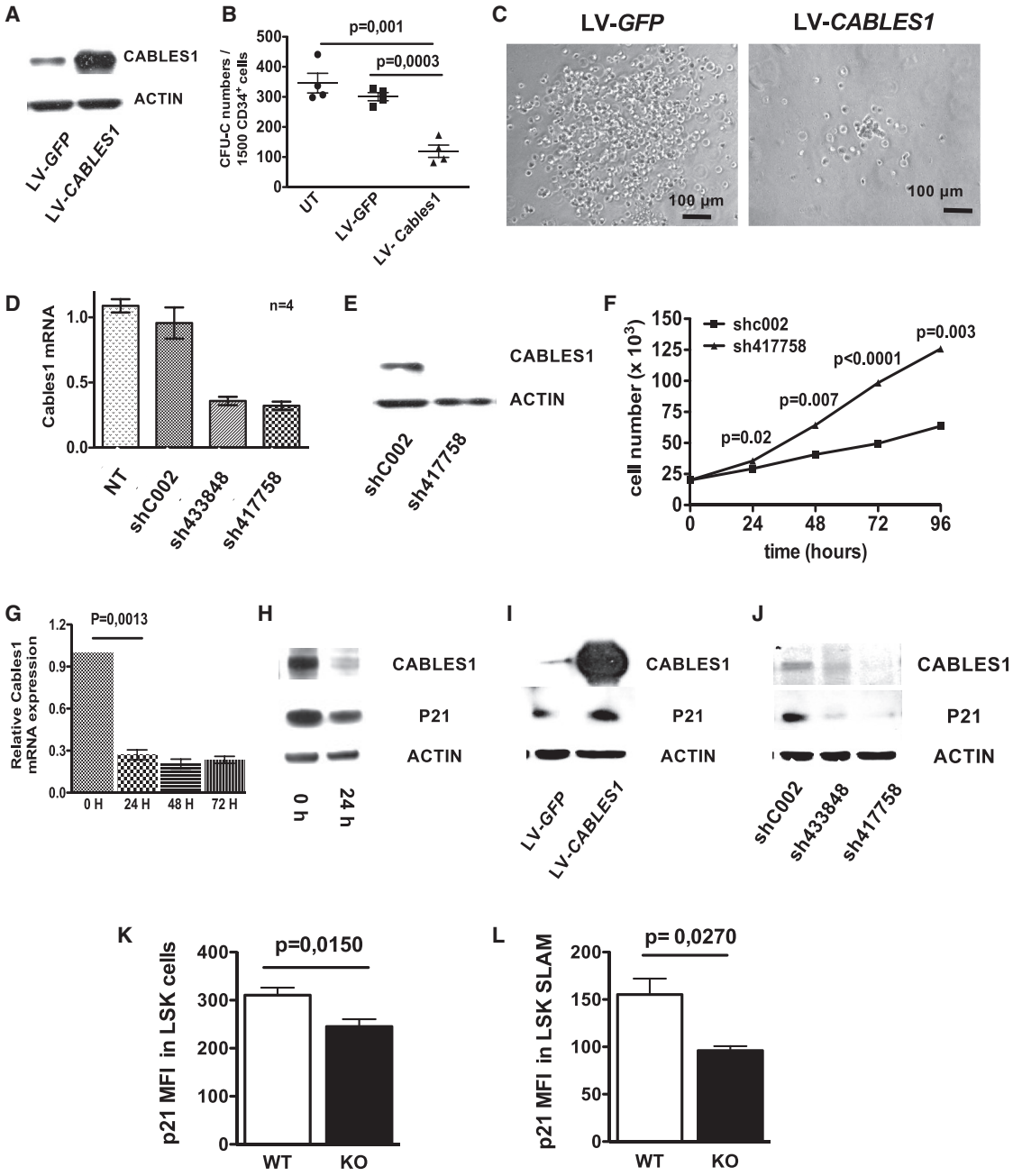

Figure 4. CABLES1 Slows Cell Growth of Human CD34$^+$ Cells and Regulates p21 Level

(A) Lentiviral overexpression of human CABLES1 in CB CD34$^+$ cells. See also Figure S5.

(B) Forty-eight hours after transduction, GFP$^+$ CD34$^+$ cells were seeded in semisolid media for CFU-C determination. Data represent the mean ± SEM of three independent experiments.

(C) Microscopic picture of colonies formed by control vector transduced CB-CD34$^+$ cells (left) and CABLES1-overexpressing CB-CD34$^+$ cells (right).

(D) CABLES1 expression in *CABLES1* shRNA-transduced CB-CD34$^+$ cells compared with cells transduced with control shRNA (shC002) and to non-transduced cells (NT). Data represent the mean ± SEM of three independent experiments.

(E) CABLES1 protein level after transduction of CB-CD34$^+$ cells with sh417758 compared with shC002.

(F) Proliferation of CB-CD34$^+$ cells after transduction with sh417758 compared with shC002. Data represent the mean ± SEM of three independent experiments.

(legend continued on next page)

Loss of Cables1 Delays Hematopoietic Regeneration after 5-FU Treatment

Recent reports suggest that p21 regulates progenitor cell proliferation during periods of stress. As CABLES1 expression is correlated with p21 protein level, we reasoned that *Cables1*$^{-/-}$ mice might be more sensitive to hematopoietic injury, for example the chemotherapy agent 5-fluorouracil (5-FU) or irradiation. Therefore, 3-month-old *Cables1*$^{-/-}$ and littermate control mice were treated with a single dose of 5-FU (250 mg/kg body weight). In treated *Cables1*$^{-/-}$ mice, WBC (Figure 5A) recovery was delayed. In addition, 10 days after 5-FU challenge, the BM of *Cables1*$^{-/-}$ mice was hypocellular, characterized by a paucity of hematopoietic clusters in both osteoblastic and vascular zones compared with the BM of *Cables1*$^{+/+}$ mice (Figures 5B and 5C). Hematopoietic clusters were seen in close contact to the bone osteoblastic zone. In line with an impaired hematopoietic recovery, progenitor cell numbers were lower in the BM (Figure 5D), spleen (Figure 5E), and blood (Figure 5F) of *Cables1*$^{-/-}$ mice. Similar results were obtained when mice were challenged with cyclophosphamide (Figures S6A–S6D) or using moderate doses of ionizing radiation (Figure S6E). Therefore, CABLES1 expression favors hematopoietic recovery in response to hematopoietic stress.

Loss of Cables1 Is Associated with Defective Hematopoiesis over Time

Given the impact of CABLES1 on hematopoietic recovery under hematopoietic stress conditions and the inability of *Cables1*-deficient HSCs to tolerate stress, we expected that CABLES1 might play a prominent role during aging. Interestingly, aged (21-month-old) *Cables1*$^{-/-}$ mice displayed a significant increase in WBC counts compared with age-matched controls, while young (3-month-old) or middle-aged (8-month-old) *Cables1*$^{-/-}$ mice had WBC numbers similar to those of their counterparts (Figure 6A). No significant changes in RBC and platelet counts were observed between *Cables1*-deficient mice and their controls during the process of aging (data not shown). It has been documented that the frequencies of B cell precursors within the BM are markedly diminished by 4–5 months of age in mice. However, paradoxically, this is not accompanied by a similar decline in the mature cells at the periphery due to compensatory mechanisms such as increased lifespan of B cells (Kline et al., 1999) (Johnson et al., 2002). In line with this, differential analysis of blood cells of *Cables1*$^{+/+}$ animals showed no significant variations in the percentage of circulating B lymphocytes during aging (Figures 6B, 6C, and S3D). However, we observed a significant decrease in the B cell percentages in 21-month-old *Cables1*$^{-/-}$-deficient mice compared with age-matched controls (Figure 6B). In contrast, the percentage of circulating mature myeloid cells (Gr-1^{+}) was significantly increased, making this cell population accountable for the increase in total leukocyte counts. No significant differences in WBC subtypes in middle-aged animals were observed between both genotypes (Figure 6C). We next wondered whether *Cables1*$^{-/-}$ progenitor cell compartments were likewise perturbed during aging. There were no differences in BM cellularity between WT and *Cables1*$^{-/-}$ mice during aging (Figure S7). However, BM clonogenic progenitor, LSK cell, and SLAM cell numbers were increased in middle-aged *Cables1*$^{-/-}$ mice compared with age-matched controls (Figures 6D–6F). Strikingly, the number of these progenitors and LSK and LSK SLAM cells was reduced in aged *Cables1*$^{-/-}$ mice compared with age-matched controls (Figures 6D–6F). Consistent with the results from young animals, LSK cells from middle-aged *Cables1*$^{-/-}$ mice displayed a significantly higher proliferation rate than their WT counterparts (Figure 6G). Of importance, the frequency of dividing cells (BrdU^{+}) within BM SLAM cells was higher in *Cables1*$^{-/-}$ mice compared with WT controls (Figure 6H).

To investigate the consequences of quiescence loss in *Cables1*$^{-/-}$ HSC, we studied the effect of a weekly injection of 5-FU. 5-FU injection induces myeloablation by preferentially eliminating actively cycling cells, which in turn activates quiescent stem cells to restore the ablated hematopoietic system. Thus weekly injection of 5-FU leads to HSC depletion, resulting in death of the mice due to BM failure. Strikingly, *Cables1*$^{-/-}$ mice had an increased sensitivity to serial 5-FU treatment and showed a decreased median survival compared with WT animals (Figure 6I). Finally, no significant differences in the number of apoptotic annexin V^{+}/DAPI^{-} cells within hematopoietic progenitor cells were detectable (data not shown), excluding that differences in apoptosis contributed to the elevated number of HSCs found in the BM of middle-aged *Cables1*$^{-/-}$ mice. Preferential differentiation into myeloid cells with loss of support for the B cell lineage is one of the characteristics

(G) *CABLES1* mRNA expression in cultured CB-CD34^{+} cells. Values are expressed as mean ± SEM; Student's unpaired two-tailed t test was performed for statistical analysis. Experiments were performed twice.
(H) Protein levels of CABLES1 and p21 in CB-CD34^{+} cells 24 h after culture.
(I) Protein levels of CABLES1 and p21 in CB-CD34^{+} cells overexpressing CABLES1.
(J) Protein levels of CABLES1 and p21 in CB-CD34^{+} cells transduced with *CABLES1* shRNAs.
(K and L) Mean fluorescence intensity (MFI) of p21 in BM LSK (K) and SLAM (L) cells of 12-week-old WT and *Cables1*$^{-/-}$ mice. Data are mean ± SEM from six mice per group, pooled from two independent experiments.

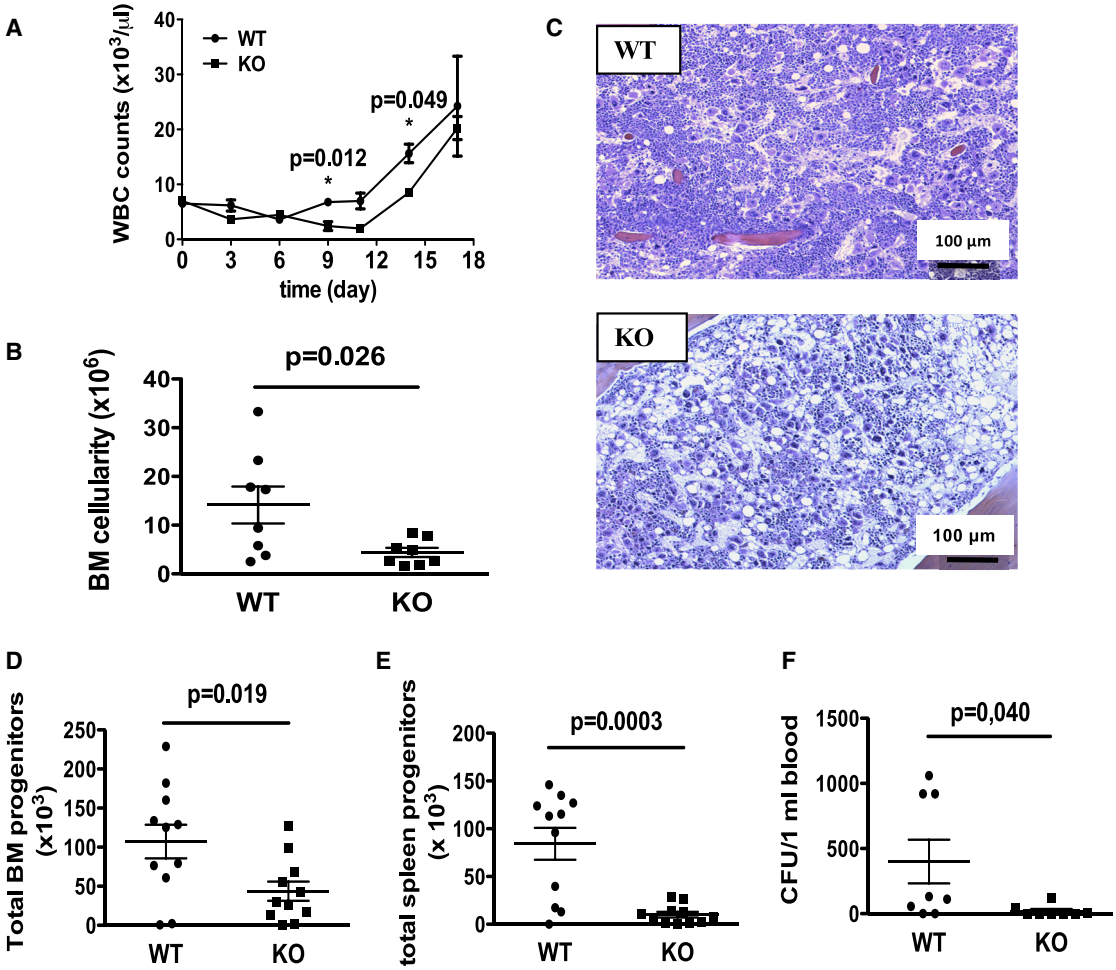

Figure 5. Loss of *Cables1* Delays Hematopoietic Regeneration after 5-FU Treatment

Three-month-old *Cables1*$^{-/-}$ and WT mice were treated with a single dose of 5-FU (250 mg/kg body weight).

(A) WBC counts (3–5 mice for each time point).

(B) BM cellularity of WT and *Cables1*$^{-/-}$ mice 10 days after 5-FU treatment.

(C) Microscopic images of BM from WT and *Cables1*$^{-/-}$ mice 10 days after 5-FU treatment. See also Figure S6.

(D–F) Total numbers of CFU-C in (D) BM, (E) spleen, and (F) blood of 5-FU-treated WT and *Cables1*$^{-/-}$ mice.

Values are mean ± SEM; Student's unpaired two-tailed t test was performed for statistical analysis.

of aged hematopoiesis (Dykstra et al., 2011). Therefore, we asked whether *Cables1*$^{-/-}$ HSCs displayed an aging-like phenotype using the CD41 and CD150 markers as previously described (Gekas and Graf, 2013). Of note, the relative frequency of myeloid-biased HSCs phenotypically defined by positive expression of CD41 in CD150^{+} LSK cell population was higher in aged *Cables1*$^{-/-}$ mice compared with WT mice (Figure 6J). We also analyzed the frequency of the LSK/CD34^{+}/CD135^{+} cell population, which is enriched for the lymphoid-primed multipotent progenitors. No difference was found between the two genotypes (Figure 6K). Similarly, the numbers of CLPs were comparable between the two genotypes (Figure 6L). In searching for the source of hematopoietic abnormalities, we assessed CFC frequency in blood and an extramedullary hematopoietic site, the spleen. Notably, both middle-aged and 21-month-old *Cables1*-deficient mice displayed increased CFU-C frequencies in blood (Figure 6M) and spleen (Figure 6N) compared with age-matched controls. Since increased mobilization could be explained by an abnormal response to CXCL12 (Foudi et al., 2006), the main chemokine involved in retention of progenitor cells within the BM, *in vitro* chemotactic assays in response to CXCL12 were performed. No significant difference was observed between the two genotypes (Figure S5D). In addition, CABLES1 overexpression in U937 and HL-60 cells did

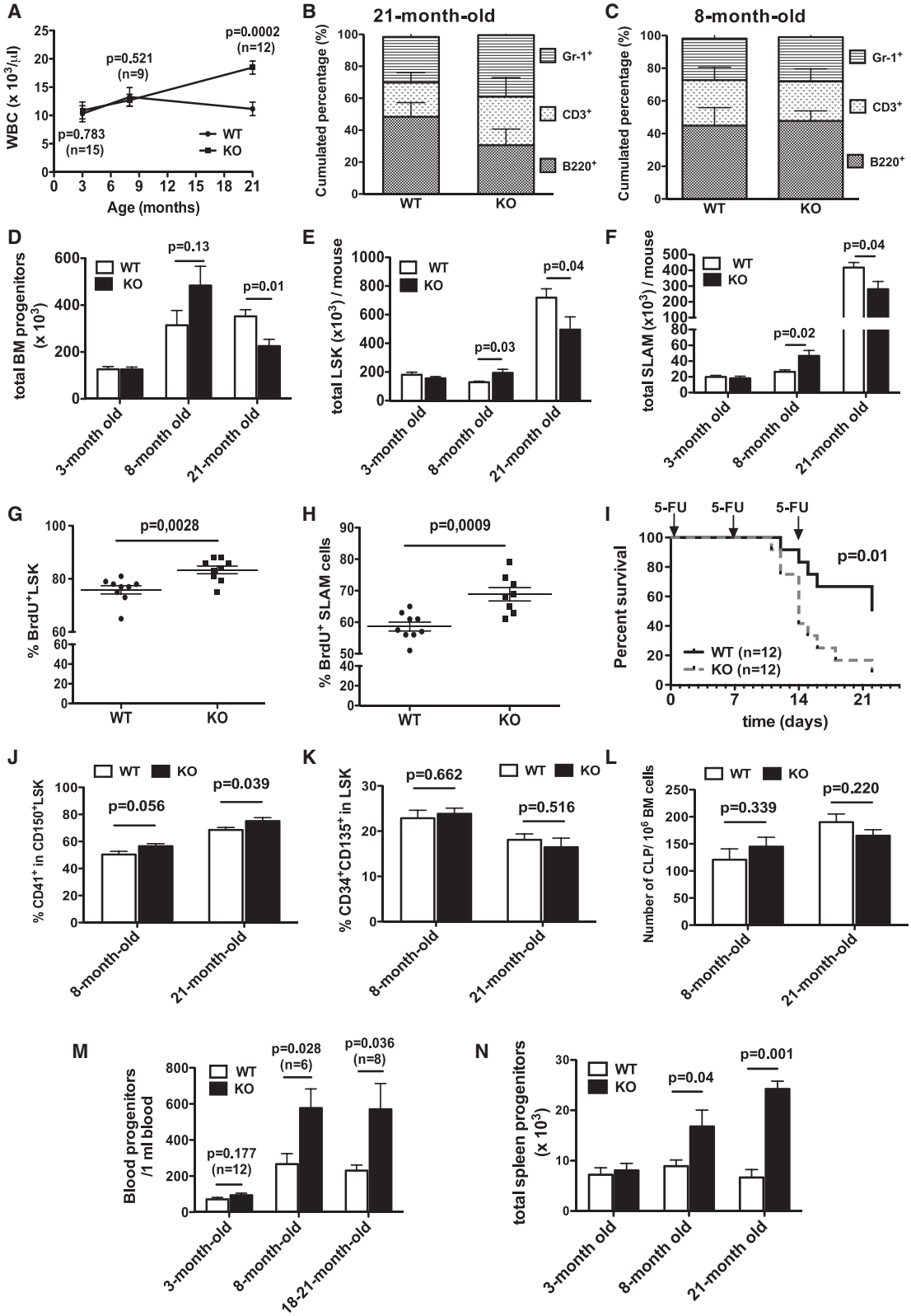

(legend on next page)

not modify their chemotactic response to CXCL12 (Figures S5E and S5F). Overall, our data demonstrate that the loss of *Cables1* is associated with defects in blood counts, HSC activation, and hematopoietic stem and progenitor cell mobilization during aging.

Environmental Defects Are Involved in the Defective Hematopoiesis of *Cables1*$^{-/-}$ Mice

Since our results showed significant CABLES1 expression in BM niche cells, we next investigated the putative role of the BM microenvironment in abnormal hematopoiesis of *Cables1*$^{-/-}$ mice. We thus conducted transplantation assays in which lethally irradiated *Cables1*$^{-/-}$ or littermate control mice were used as recipients for WT CD45.1^{+} transplant BM cells (Figure 7A). Four months after reconstitution, *Cables1*$^{-/-}$ recipient mice displayed a significant decrease in relative B cell donor counts with a significant increase in the frequency of mature myeloid cells (Figures 7B and 7C). We also determined whether the increased susceptibility of *Cables1*$^{-/-}$ mice to serial 5-FU injection was cell autonomous or related to an abnormal microenvironment. *Cables1*$^{-/-}$ or WT BM cells were transplanted into lethally irradiated recipients of both genetic backgrounds in order to obtain chimeric mice. Four months after hematopoietic reconstitution, 5-FU was injected three times at 10-day intervals and survival was monitored (Figure 7D). As expected, most (12/13) *Cables1*$^{-/-}$/*Cables1*$^{-/-}$ mice died after 5-FU treatment while fewer WT/WT mice (4/12) succumbed, recapitulating our observation in middle-aged straight *Cables1*$^{-/-}$ mice. Conversely, *Cables1*$^{-/-}$ recipient mice reconstituted with either *Cables1*$^{+/+}$ or *Cables1*$^{-/-}$ BM cells showed a decreased median survival, compared with *Cables1*$^{+/+}$ recipient mice reconstituted with WT or *Cables1*$^{-/-}$ BM cells. Of note, *Cables1*$^{-/-}$ recipient mice reconstituted with either *Cables1*$^{-/-}$ or WT BM cells showed no significant difference in survival curves, and this was also observed for WT recipient groups transplanted with *Cables1*$^{-/-}$ or littermate control BM cells. Overall, these results indicate that the lack of *Cables1* in hematopoietic cells is not sufficient to provide a disadvantage to mice treated with repeated cycles of 5-FU, and suggest that the increased susceptibility of *Cables1*$^{-/-}$ mice to 5-FU is mainly related to an abnormal hematopoietic microenvironment. To substantiate this finding, we quantified the mesenchymal stromal progenitor cells in the BM of *Cables1*$^{-/-}$ and *Cables1*$^{+/+}$ mice by CFU-fibroblast (CFU-F) assays. CFU-F frequencies were comparable in the BM of 3-month-old mice (Figure 7E). However, middle-aged and aged *Cables1*$^{-/-}$ mice displayed a lower frequency of CFU-F compared with their age-matched counterparts (Figures 7F and 7G). These data show that the BM microenvironment is altered in *Cables1*$^{-/-}$ during aging. Altogether, our results indicate that CABLES1 plays both intrinsic and extrinsic roles in hematopoiesis, as summarized in Figure 7H.

DISCUSSION

Here, we report that CABLES1 plays at least two important roles in the regulation of the HSC pool. One of these is cell autonomous, mainly evidenced in stress conditions; the second role relates to the microenvironment and underscores the role of CABLES1 during aging of HSCs.

The first preliminary evidence for a role of CABLES1 in the regulation of hematopoiesis came from the observation that the number of progenitor cells was slightly increased in the BM of *Cables1*$^{-/-}$ mice (Lee et al., 2007). Our data revealed that the cell-cycle status of HSCs was not altered in steady-state young animals. In contrast, we revealed an enhanced proliferative status of HSCs when transplanted into WT recipients, suggesting that enhanced proliferation of *Cables1*$^{-/-}$ HSCs may operate preferentially during hematopoietic stress. This could explain the slightly higher competitive characteristics of *Cables1*$^{-/-}$ HSCs over their WT counterparts. *Cables1*$^{-/-}$ HSCs displayed higher reconstitution fitness despite hyperproliferation

Figure 6. Loss of *Cables1* Is Associated with Defective Hematopoiesis in Aged Mice

(A) WBC counts in WT and *Cables1*$^{-/-}$ mice at different ages.

(B–D) WBC subtypes (B220^{+}, CD3^{+}, Gr-1^{+}) in (B) 21-month-old (n = 6) and (C) 8-month-old (n = 5) mice. (D) Total BM CFU-C numbers of 3-, 8-, and 21-month-old *Cables1*$^{-/-}$ and WT mice (n = 5–6).

(E and F) Total numbers of (E) LSK and (F) SLAM cells in 3-, 8-, and 21-month-old *Cables1*$^{-/-}$ and WT mice (n = 5–6). See also Figure S7.

(G and H) Frequencies of BrdU^{+} LSK (G) and SLAM cells (H) in 8-month-old mice after 12 days of BrdU exposure (n = 6).

(I) Survival of 8-month-old mice treated weakly with 5-FU.

(J) Percentages of myeloid-biased HSC (CD41^{+}CD150^{+}LSK) within the CD150^{+}LSK compartment in *Cables1*$^{-/-}$ and WT mice (n = 10).

(K) Frequency of BM LSK/CD34^{+}/CD135^{+} cells in *Cables1*$^{-/-}$ and WT mice (n = 10 for 8-month-old mice; n = 5 for 21-month-old mice).

(L) Frequency of CLP in BM of *Cables1*$^{-/-}$ and WT mice (n = 5).

(M and N) CFU-C numbers in blood (M) and spleen (N) of 3-, 8-, and 21-month-old *Cables1*$^{-/-}$ and WT mice (n = 6). See also Figures S5D–S5F.

Data are expressed as mean ± SEM. Log-rank (Mantel-Cox) test was applied for comparing survival between WT and *Cables1*$^{-/-}$ mice. Student's unpaired two-tailed t test was performed for the other experiments.

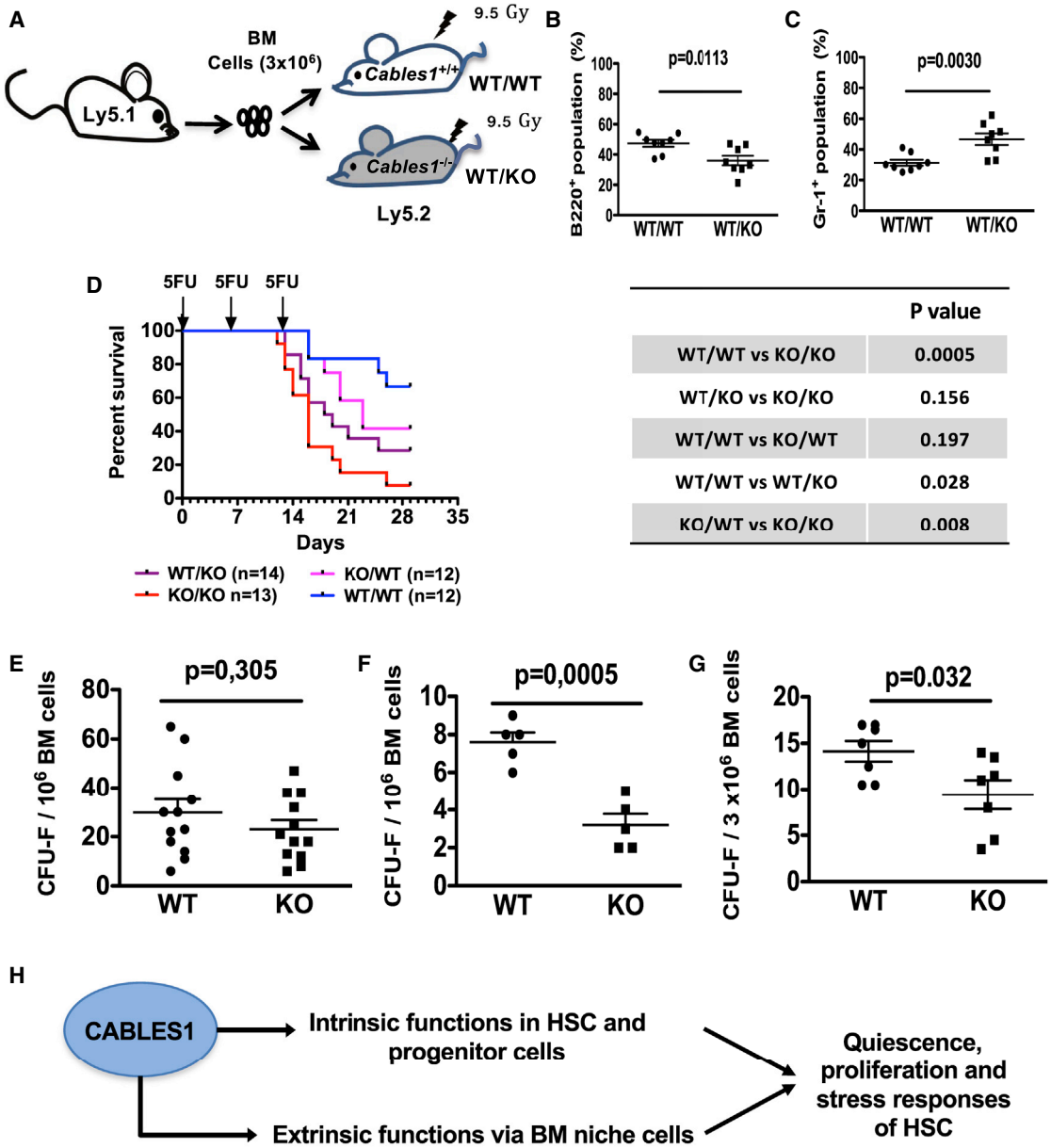

Figure 7. Environmental Defects Are Involved in Abnormal Hematopoiesis of Aged *Cables1*$^{-/-}$ Mice

(A) Schematic representation of BM transplantation.

(B and C) Frequencies of (B) donor-derived B cells (B220^{+}) and (C) myeloid cells (Gr-1^{+}) 4 months after reconstitution (n = 8).

(D) Survival of chimeric mice after weekly treatment with 5-FU. Log-rank (Mantel-Cox) test was applied for comparing survival between the different groups.

(E–G) BM CFU-F frequency of (E) 3-, (F) 8-, and (G) 21-month-old WT and *Cables1*$^{-/-}$ mice. Data are expressed as means ± SEM. Student's unpaired two-tailed t test was performed for statistical analysis.

(H) Illustrative diagram depicting the main identified roles for CABLES1.

under transplantation settings. This indicates that hyperproliferation per se does not necessarily inhibit stem cell function. In line with this, the knockout of some genes including cell-cycle regulatory genes such as Cdkn2c or Cdkn2a enables preservation or higher repopulation potential despite increased HSC proliferation (Janzen et al., 2006; Yu et al., 2006; Yuan et al., 2004). Thus, our results suggest that CABLES1 controls progenitor proliferation through a cell-autonomous mechanism and that it is required for quiescence of HSCs especially under stress conditions.

Several studies have previously demonstrated that CABLES1 is present in a multimolecular complex containing p21/Cip (Shi et al., 2015). The cyclin-dependent kinase inhibitor $p21^{Cip1/Waf1}$ is a G_1 checkpoint regulator that selectively regulates HSCs and progenitor cell behavior under stress conditions (Cheng et al., 2000a; Van Os et al., 2007). Using overexpression experiments, we showed that enhanced CABLES1 expression in human progenitor cells clearly correlated with an increase in p21 protein expression. Inversely, when an shRNA strategy was used, decreased CABLES1 expression correlated with a decrease in p21 protein expression. Mechanistically, CABLES1 interferes with proteasome subunit alpha type 3 (PMSA3) binding to p21 and protects p21 from proteasomal degradation (Shi et al., 2014). In line with these studies, we showed that p21 mRNA expression is not affected by CABLES1 expression, suggesting that CABLES1 may control p21 levels in hematopoietic cells through a post-transcriptional mechanism.

At steady state in young animals, *Cables1* deletion affected essentially the cell cycle of progenitor cells with only few effects on HSC numbers and cell cycle. Deletion of p21 has also a limited role on steady-state hematopoiesis and its impact on HSCs was only observed under stress conditions, such as 5-FU treatment and irradiation (Cheng et al., 2000b; Van Os et al., 2007) similarly to what we observed in *Cables1*$^{-/-}$ mice. Despite these similarities, our experiments revealed that the deletion of *Cables1* does not completely recapitulate the *p21* phenotype. Indeed, under transplantation settings, *Cables1*$^{-/-}$ HSCs displayed a higher proliferative status while the deletion of *p21* led to PMSA3 decreased (Cheng et al., 2000b) or normal reconstitution (Van Os et al., 2007). Thus, although these observations are consistent with the model that inhibition of proliferation by CABLES1 operates at least in part through an increase of p21 activity, other CABLES1 targets could be involved. Indeed, CABLES1 has a cyclin-like domain, which is a key element in its interactions with multiple Cdks including Cdk3, Cdk2, and Cdk5 (Matsuoka et al., 2003; Zukerberg et al., 2000). CABLES1 is phosphorylated by Cdk2 or Cdk3 bound to cyclin A and cyclin E (Yamochi et al., 2001). In addition, CABLES1 enhances Cdk2 tyrosine phosphorylation at residue 15 by Wee1 family kinase, leading to the inhibition of Cdk2 activity and suppression of cell proliferation (Wu et al., 2001). Therefore, regulation of these targets by CABLES1 can account for increased proliferative capacity of *Cables1*-deficient cells under transplantation.

By further investigating *Cables1*$^{-/-}$ mice, we observed that loss of *Cables1* is associated with defective hematopoiesis over time. At 21 months of age, *Cables1*$^{-/-}$ mice displayed a significant increase in myeloid cell numbers in the periphery without significant alterations in B cell counts. This phenotype is not transplantable, suggesting that this feature is not HSC autonomous.

To understand why *Cables1*$^{-/-}$ mice display increased 5-FU sensitivity, we conducted transplantation assays in which lethally irradiated *Cables1*$^{-/-}$ or littermate control mice were used as recipients for WT transplant BM cells. We also generated reverse chimera by transplanting *Cables1*$^{-/-}$ BM cells to irradiated *Cables1*$^{-/-}$ or littermate control mice. Using this strategy, we demonstrated that the increased susceptibility of *Cables1*$^{-/-}$ mice to 5-FU is mainly dependent on the BM microenvironment. Indeed, 5-FU not only acts on HSCs but also on niche cells that become stimulated, thus inducing a stimulating effect on HSCs (Jeong et al., 2018). Our hypothesis is supported by our results showing that niche cells, including MSCs, express high levels of *CABLES1* mRNA and protein. In addition, we have afforded evidence that BM from *Cables1*$^{-/-}$ mice have lower numbers of MSCs, indicating that CABLES1 is important for stromal cells. MSCs are the principal cells that mediate retention of progenitor cells within the BM, and their deficiency is often associated with a marked exhaustion of HSCs and increased mobilization of progenitor cells. The phenotype of middle-aged *Cables1*$^{-/-}$ mice strikingly mimicked transgenic mice with such MSC depletion. It remains to be determined how CABLES1 regulates the dynamic adaptation of niche cells to replicative stress and how this adaptation influences the regeneration of HSCs. One potential mechanism could be stress- or age-associated decreases in the adhesion potential of *Cables1*$^{-/-}$ MSCs (Rhee et al., 2007). The use of *in vitro* and *in vivo* models as described recently will help to more deeply understand how CABLES1 regulates the dynamic adaptation of niche cells to replicative stress and how this adaptation influences the regeneration of HSCs (Jeong et al., 2018).

In conclusion, we report here an important role of CABLES1 in the direct regulation of progenitor cell cycle and long-term hematopoiesis. Our results suggest that the observed defects in *Cables1*$^{-/-}$ mice may be due in part to the potential role of CABLES1 in regulating p21 levels. The present results also underscore the protective role of CABLES1 during genotoxic stress and aging.

EXPERIMENTAL PROCEDURES

Animals

Heterozygous *Cables1*$^{+/-}$ C57BL/6 (CD45.2) background mice were previously described and kindly provided by B.R.R. (Zukerberg et al., 2004). All experiments were approved by an appropriate institutional review committee (C2EA-26, Animal Care, Villejuif, France).

Culture of Human Cord Blood CD34^{+} Cells and Mesenchymal Stem Cells

CB samples from normal full-term newborn infants were collected after normal vaginal delivery with informed written consent.

$CD34^+$ cells separated using a magnetic cell-sorting system (miniMACS; Miltenyi Biotec) were cultured as previously described (Abdelouahab et al., 2017). MSCs were obtained by culture of BM from healthy donors in plastic dishes in MSC expansion medium (Miltenyi Biotech). Chemotaxis assays in response to CXCL12 were performed as previously described (Rivière et al., 1999).

Flow Cytometry

BM cells were analyzed on FACS CANTO II (Becton Dickinson) and sorted on an Influx flow cytometer (BD). HSC cell-cycle analysis was performed with either Ki67/Hoechst 33342 or BrdU/Hoechst 33342 costaining. Intracellular p21 was assessed with anti-p21 antibody (Thermo Fisher Scientific) followed by a goat anti-rabbit AlexaFluor 488 antibody, according to the supplied protocol of fixation/permeabilization BD Cytofix/Cytoperm. Mitochondrial ROS detection was assessed after staining for 20 min with 10 μM Mitosox at 37°C as previously described (Zhang et al., 2016). BM cells stained for surface markers were incubated with AlexaFluor 647-conjugated annexin V (Invitrogen) and DAPI, according to the supplied protocol. To avoid false-positive annexin V staining, we processed cells at 2°C–8°C and analyzed them within 4 h after recovery from mice.

Reconstitution Assays

To establish chimeric mice, we lethally irradiated 12- to 14-week-old *Cables1*$^{-/-}$ and *Cables1*$^{+/+}$ mice and 24 h later, mice were reconstituted with 5 × 10^6 *Cables1*$^{-/-}$ or *Cables1*$^{+/+}$ BM cells from 8- to 10-week-old mice. The reconstitution was analyzed by sampling blood once per month. Mice were euthanized 5 months after transplantation for analyzing test cell-derived HSCs and their cycling status by Ki67 assay. Half of the spleen and one femur per mouse were kept for immunohistochemistry.

For competitive assays, cells (3 × 10^6 BM cells/host) from *Cables1*$^{-/-}$ and *Cables1*$^{+/+}$ donor mice (CD45.2) and an equal number of CD45.1 BM cells (competitor cells) were co-transplanted into lethally irradiated (9.5 Gy) CD45.1 recipients. Blood was collected monthly after transplantation, and the relative contribution of test cells (CD45.2) to competitor cells (CD45.1) in the reconstituted host was quantified by flow cytometry. For reconstitution with purified cells, WT or KO BM LSK cells (8,000 cells per mouse) were injected together with 1.5 × 10^5 CD45.1 BM cells.

Treatment of Mice with 5-FU or LPS

Mice were injected intraperitoneally with 5-FU (Fluorouracil Dakota Pharm, Paris, France) at 150 mg/kg body weight for survival rates of mice or at 250 mg/kg body weight for hematopoietic regeneration analysis. Mice were treated with 4 mg of cyclophosphamide followed by 5 days of 5 μg of recombinant human (rh) granulocyte-colony stimulating factor per day subcutaneously. *Cables1*$^{-/-}$ and *Cables1*$^{+/+}$ mice were subjected to TBI (6 Gy). Mice were injected with LPS (200 μg/kg body weight) and sacrificed 24 h later.

Transduction of Human CB $CD34^+$ Cells

Human *CABLES1* cDNA sequence was cloned into the lentiviral vector pTrip-MND-IRES-GFP vector (kindly provided by F. Pflumio, CEA, L'Hay-les-Roses, France). *CABLES1* shRNAs (417758, 433848) and the control shc002, all from Sigma, were cloned into a lentiviral vector (pRRLsin-PGK-eGFP-WPRE, Genethon). Cell transduction was performed as previously described (Hirsch et al., 2016). To test the effect of CABLES1 overexpression on $CD34^+$ cell proliferation, we sorted 4,000 GFP^+ cells 48 h after transduction and seeded them in human methylcellulose supplemented with rh stem cell factor (50 ng/mL, Biovitrum, Stockholm, Sweden), rh interleukin-3 (100 U/mL, Peprotech, France), and rh erythropoietin (1 U/mL, Amersham). Colonies were counted after 2 weeks.

Data Processing and Statistical Analysis

Flow-cytometry results were analyzed by BD FACS Diva software. Results were evaluated using Student's unpaired t test by GraphPad Prism version 5.0 (GraphPad Software, San Diego, CA, USA). Results are presented as means ± SEM and the value of $p < 0.05$ was determined as significant, with $p < 0.01$ and $p < 0.001$ highly significant.

SUPPLEMENTAL INFORMATION

Supplemental Information can be found online at https://doi.org/10.1016/j.stemcr.2019.06.002.

AUTHOR CONTRIBUTIONS

H.L. performed experiments, analyzed data and wrote the paper. F.B., V.B., M.D., Y.Z., and M.W. performed experiments and analyzed data. A.F., V.J., B.R.R., and P.G. analyzed data. F.L. designed and supervised the study, analyzed data, and wrote the manuscript. All authors contributed to writing and editing.

ACKNOWLEDGMENTS

This work was supported by Institut National de la Santé et de la Recherche Médicale and grants from Ligue Contre le Cancer (DM/CB/004-17) and ARC (PJA 20161204702) to F.L. Y.Z. was supported by Cancéropole, Ile de France. We thank P. Rameau, Y. Lecluse, and Cyril Catelain for flow cell sorting, O. Bawa for immunohistochemistry, and the staff of the animal facility, M. Ganga, L. Touchard, and G. Joussard, for excellent animal care.

Received: August 14, 2018
Revised: June 14, 2019
Accepted: June 17, 2019
Published: July 18, 2019

REFERENCES

Abdelouahab, H., Zhang, Y., Wittner, M., Oishi, S., Fujii, N., Besancenot, R., Plo, I., Ribrag, V., Solary, E., Vainchenker, W., et al. (2017). CXCL12/CXCR4 pathway is activated by oncogenic JAK2 in a PI3K-dependent manner. Oncotarget *8*, 54082–54095.

Arnason, T., Pino, M.S., Yilmaz, O., Kirley, S.D., Rueda, B.R., Chung, D.C., and Zukerberg, L.R. (2013). *Cables1* is a tumor suppressor gene that regulates intestinal tumor progression in ApcMin mice. Cancer Biol. Ther. *14*, 672–678.

Bernitz, J.M., Kim, H.S., MacArthur, B., Sieburg, H., and Moore, K. (2016). Hematopoietic stem cells count and remember self-renewal divisions. Cell *167*, 1296–1309.e10.

Cheng, T., Rodrigues, N., Dombkowski, D., Stier, S., and Scadden, D.T. (2000a). Stem cell repopulation efficiency but not pool size is governed by p27(kip1). Nat. Med. *6*, 1235–1240.

Cheng, T., Rodrigues, N., Shen, H., Yang, Y., Dombkowski, D., Sykes, M., and Scadden, D.T. (2000b). Hematopoietic stem cell quiescence maintained by p21cip1/waf1. Science *287*, 1804–1809.

DeBernardo, R.L., Littell, R.D., Luo, H., Duska, L.R., Oliva, E., Kirley, S.D., Lynch, M.P., Zukerberg, L.R., and Rueda, B.R. (2005). Defining the extent of CABLES loss in endometrial cancer subtypes and its effectiveness as an inhibitor of cell proliferation in malignant endometrial cells in vitro and in vivo. Cancer Biol. Ther. *4*, 103–107.

Dong, Q., Kirley, S., Rueda, B., Zhao, C., Zukerberg, L., and Oliva, E. (2003). Loss of *CABLES*, a novel gene on chromosome 18q, in ovarian cancer. Mod. Pathol. *16*, 863–868.

Dykstra, B., Olthof, S., Schreuder, J., Ritsema, M., and de Haan, G. (2011). Clonal analysis reveals multiple functional defects of aged murine hematopoietic stem cells. J. Exp. Med. *208*, 2691–2703.

Florian, M.C., Dorr, K., Niebel, A., Daria, D., Schrezenmeier, H., Rojewski, M., Filippi, M.-D., Hasenberg, A., Gunzer, M., Scharffetter-Kochanek, K., et al. (2012). Cdc42 activity regulates hematopoietic stem cell aging and rejuvenation. Cell Stem Cell *10*, 520–530.

Foudi, A., Jarrier, P., Zhang, Y., Wittner, M., Geay, J.F., Lecluse, Y., Nagasawa, T., Vainchenker, W., and Louache, F. (2006). Reduced retention of radioprotective hematopoietic cells within the bone marrow microenvironment in *Cxcr4*$^{-/-}$ chimeric mice. Blood *107*, 2243–2251.

Foudi, A., Hochedlinger, K., Van Buren, D., Schindler, J.W., Jaenisch, R., Carey, V., and Hock, H. (2009). Analysis of histone 2B-GFP retention reveals slowly cycling hematopoietic stem cells. Nat. Biotechnol. *27*, 84–90.

Gekas, C., and Graf, T. (2013). CD41 expression marks myeloid-biased adult hematopoietic stem cells and increases with age. Blood *121*, 4463–4472.

Groeneweg, J.W., White, Y.A.R., Kokel, D., Peterson, R.T., Zukerberg, L.R., Berin, I., Rueda, B.R., and Wood, A.W. (2011). CABLES1 is required for embryonic neural development: molecular, cellular, and behavioral evidence from the zebrafish. Mol. Reprod. Dev. *78*, 22–32.

Hirsch, P., Zhang, Y., Tang, R., Joulin, V., Boutroux, H., Pronier, E., Moatti, H., Flandrin, P., Marzac, C., Bories, D., et al. (2016). Genetic hierarchy and temporal variegation in the clonal history of acute myeloid leukaemia. Nat. Commun. *7*, 12475.

Huang, J.-R., Tan, G.-M., Li, Y., and Shi, Z. (2017). The emerging role of CABLES1 in cancer and other diseases. Mol. Pharmacol. *92*, 240–245.

Janzen, V., Forkert, R., Fleming, H.E., Saito, Y., Waring, M.T., Dombkowski, D.M., Cheng, T., DePinho, R.A., Sharpless, N.E., and Scadden, D.T. (2006). Stem-cell ageing modified by the cyclin-dependent kinase inhibitor p16INK4a. Nature *443*, 421–426.

Jeong, S.Y., Kim, J.A., and Oh, I.H. (2018). The adaptive remodeling of stem cell niche in stimulated bone marrow counteracts the leukemic niche. Stem Cells *36*, 1617–1629.

Johnson, K.M., Owen, K., and Witte, P.L. (2002). Aging and developmental transitions in the B cell lineage. Int. Immunol. *14*, 1313–1323.

Kiel, M.J., Yilmaz, Ö.H., Iwashita, T., Yilmaz, O.H., Terhorst, C., and Morrison, S.J. (2005). SLAM family receptors distinguish hematopoietic stem and progenitor cells and reveal endothelial niches for stem cells. Cell *121*, 1109–1121.

Kline, G.H., Hayden, T.A., and Klinman, N.R. (1999). B cell maintenance in aged mice reflects both increased B cell longevity and decreased B cell generation. J. Immunol. *162*, 3342–3349.

Lee, H.J., Sakamoto, H., Luo, H., Skaznik-Wikiel, M.E., Friel, A.M., Niikura, T., Tilly, J.C., Niikura, Y., Klein, R., Styer, A.K., et al. (2007). Loss of CABLES1, a cyclin-dependent kinase-interacting protein that inhibits cell cycle progression, results in germline expansion at the expense of oocyte quality in adult female mice. Cell Cycle *6*, 2678–2684.

Matsuoka, M., Sudo, H., Tsuji, K., Sato, H., Kurita, M., Suzuki, H., Nishimoto, I., and Ogata, E. (2003). ik3-2, a relative to ik3-1/CABLES, is involved in both p53-mediated and p53-independent apoptotic pathways. Biochem. Biophys. Res. Commun. *312*, 520–529.

Mendez-Ferrer, S., Scadden, D.T., and Sanchez-Aguilera, A. (2015). Bone marrow stem cells: current and emerging concepts. Ann. N. Y. Acad. Sci. *1335*, 32–44.

Morita, Y., Ema, H., and Nakauchi, H. (2010). Heterogeneity and hierarchy within the most primitive hematopoietic stem cell compartment. J. Exp. Med. *207*, 1173–1182.

Orkin, S.H., and Zon, L.I. (2008). Hematopoiesis: an evolving paradigm for stem cell biology. Cell *132*, 631–644.

Van Os, R., Kamminga, L.M., Ausema, A., Bystrykh, L.V., Draijer, D.P., van Pelt, K., Dontje, B., and de Haan, G. (2007). A limited role for p21Cip1/Waf1 in maintaining normal hematopoietic stem cell functioning. Stem Cells *25*, 836–843.

Park, D.Y., Sakamoto, H., Kirley, S.D., Ogino, S., Kawasaki, T., Kwon, E., Mino-Kenudson, M., Lauwers, G.Y., Chung, D.C., Rueda, B.R., et al. (2007). The *CABLES* gene on chromosome 18q is silenced by promoter hypermethylation and allelic loss in human colorectal cancer. Am. J. Pathol. *171*, 1509–1519.

Pietras, E.M., Lakshminarasimhan, R., Techner, J.-M., Fong, S., Flach, J., Binnewies, M., and Passegue, E. (2014). Re-entry into quiescence protects hematopoietic stem cells from the killing effect of chronic exposure to type I interferons. J. Exp. Med. *211*, 245–262.

Rhee, J., Buchan, T., Zukerberg, L., Lilien, J., and Balsamo, J. (2007). CABLES links Robo-bound Abl kinase to N-cadherin-bound beta-catenin to mediate Slit-induced modulation of adhesion and transcription. Nat. Cell Biol. *9*, 883–892.

Rivière, C., Subra, F., Cohen-Solal, K.A., Cordette-Lagarde, V., Letestu, R., Auclair, C., Vainchenker, W., and Louache, F. (1999). Phenotypic and functional evidence for the expression of CXCR4 receptor during megakaryocytopoiesis. Blood *93*, 1689–1699.

Rossi, D.J., Bryder, D., Zahn, J.M., Ahlenius, H., Sonu, R., Wagers, A.J., and Weissman, I.L. (2005). Cell intrinsic alterations underlie

hematopoietic stem cell aging. Proc. Natl. Acad. Sci. U S A *102*, 9194–9199.

Shi, Z., Li, Z., Li, Z.J., Cheng, K., Du, Y., Fu, H., and Khuri, F.R. (2014). CABLES1 controls p21/Cip1 protein stability by antagonizing proteasome subunit alpha type 3. Oncogene *34*, 2538–2545.

Shi, Z., Park, H.R., Du, Y., Li, Z., Cheng, K., Sun, S.Y., Li, Z., Fu, H., and Khuri, F.R. (2015). CABLES1 complex couples survival signaling to the cell death machinery. Cancer Res. *75*, 147–158.

Tsuji, K., Mizumoto, K., Yamochi, T., Nishimoto, I., and Matsuoka, M. (2002). Differential effect of ik3-1/CABLES on p53- and p73-induced cell death. J. Biol. Chem. *277*, 2951–2957.

Wu, C.L., Kirley, S.D., Xiao, H., Chuang, Y., Chung, D.C., and Zukerberg, L.R. (2001). CABLES enhances cdk2 tyrosine 15 phosphorylation by Wee1, inhibits cell growth, and is lost in many human colon and squamous cancers. Cancer Res. *61*, 7325–7332.

Yamochi, T., Semba, K., Tsuji, K., Mizumoto, K., Sato, H., Matsuura, Y., Nishimoto, I., and Matsuoka, M. (2001). ik3-1/CABLES is a substrate for cyclin-dependent kinase 3 (cdk 3). Eur. J. Biochem. *268*, 6076–6082.

Yu, H., Yuan, Y., Shen, H., and Cheng, T. (2006). Hematopoietic stem cell exhaustion impacted by p18 INK4C and p21 Cip1/Waf1 in opposite manners. Blood *107*, 1200–1206.

Yuan, Y., Shen, H., Franklin, D.S., Scadden, D.T., and Cheng, T. (2004). In vivo self-renewing divisions of haematopoietic stem cells are increased in the absence of the early G1-phase inhibitor, p18INK4C. Nat. Cell Biol. *6*, 436–442.

Zhang, Y., Dépond, M., He, L., Foudi, A., Kwarteng, E.O., Lauret, E., Plo, I., Desterke, C., Dessen, P., Fujii, N., et al. (2016). CXCR4/CXCL12 axis counteracts hematopoietic stem cell exhaustion through selective protection against oxidative stress. Sci. Rep. *6*, 37827.

Zukerberg, L.R., Patrick, G.N., Nikolic, M., Humbert, S., Wu, C.-L., Lanier, L.M., Gertler, F.B., Vidal, M., Van Etten, R.A., and Tsai, L.-H. (2000). CABLES links Cdk5 and c-Abl and facilitates Cdk5 tyrosine phosphorylation, kinase upregulation and neurite outgrowth. Neuron *26*, 633–646.

Zukerberg, L.R., DeBernardo, R.L., Kirley, S.D., D'Apuzzo, M., Lynch, M.P., Littell, R.D., Duska, L.R., Boring, L., and Rueda, B.R. (2004). Loss of CABLES, a cyclin-dependent kinase regulatory protein, is associated with the development of endometrial hyperplasia and endometrial cancer. Cancer Res. *64*, 202–208.

Stem Cell Reports, Volume *13*

Supplemental Information

CABLES1 Deficiency Impairs Quiescence and Stress Responses of Hematopoietic Stem Cells in Intrinsic and Extrinsic Manners

Liang He, Florian Beghi, Viviane Baral, Mallorie Dépond, Yanyan Zhang, Virginie Joulin, Bo R. Rueda, Patrick Gonin, Adlen Foudi, Monika Wittner, and Fawzia Louache

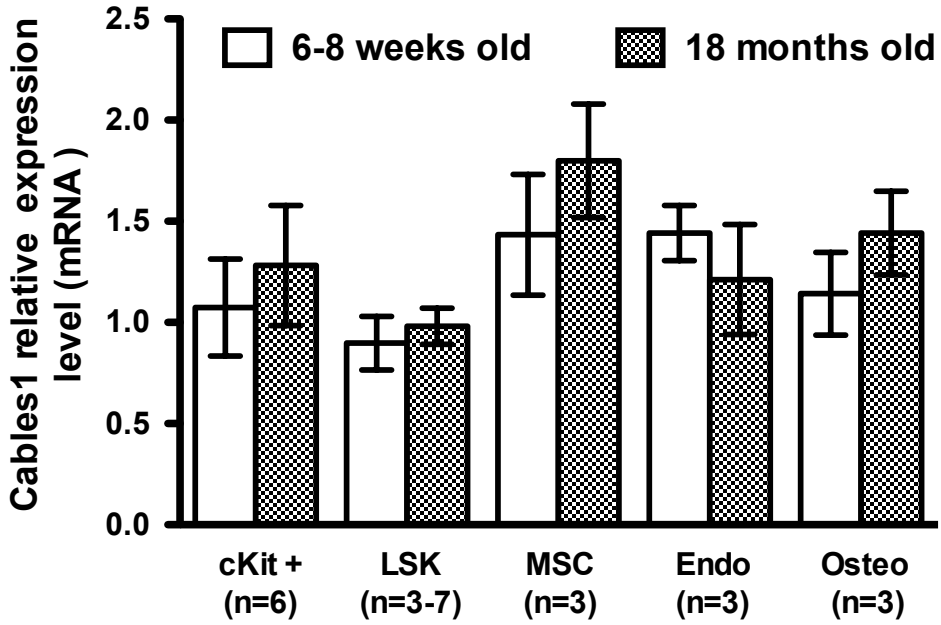

Figure S1: *Cables1* mRNA expression in murine immature hematopoietic and niche cells during aging. Young (6-8 weeks old) and 18 month-old mice were used. Lin^- (lineage markers negative cells, namely $CD3^-B220^-Ter119^-Gr\text{-}1^-$), LSK ($Lin^-c\text{-}Kit^+Sca\text{-}1^+$) and $c\text{-}kit^+$ ($Lin^-c\text{-}Kit^+Sca\text{-}1^-$) cells were sorted by fluorescence-activated cell sorting (FACS). After bone digestion, cellular components of the hematopoietic microenvironment – osteoblasts ($CD45^-Ter119^-CD31^-Sca\text{-}1^-CD51^+$), endothelial cells ($CD45^-Ter119^-CD31^+$), and MSC (mesenchymal stem cells ($CD45^-Ter119^-/CD31^-Sca^+CD51^+$) were also sorted by FACS. Expression levels were normalized to Hprt transcript levels. FACS purified c-kit positive cells served as reference to standardize for relative expression. Data are expressed as mean ± SEM, Student's two-tailed unpaired t-test was performed for statistical analysis.

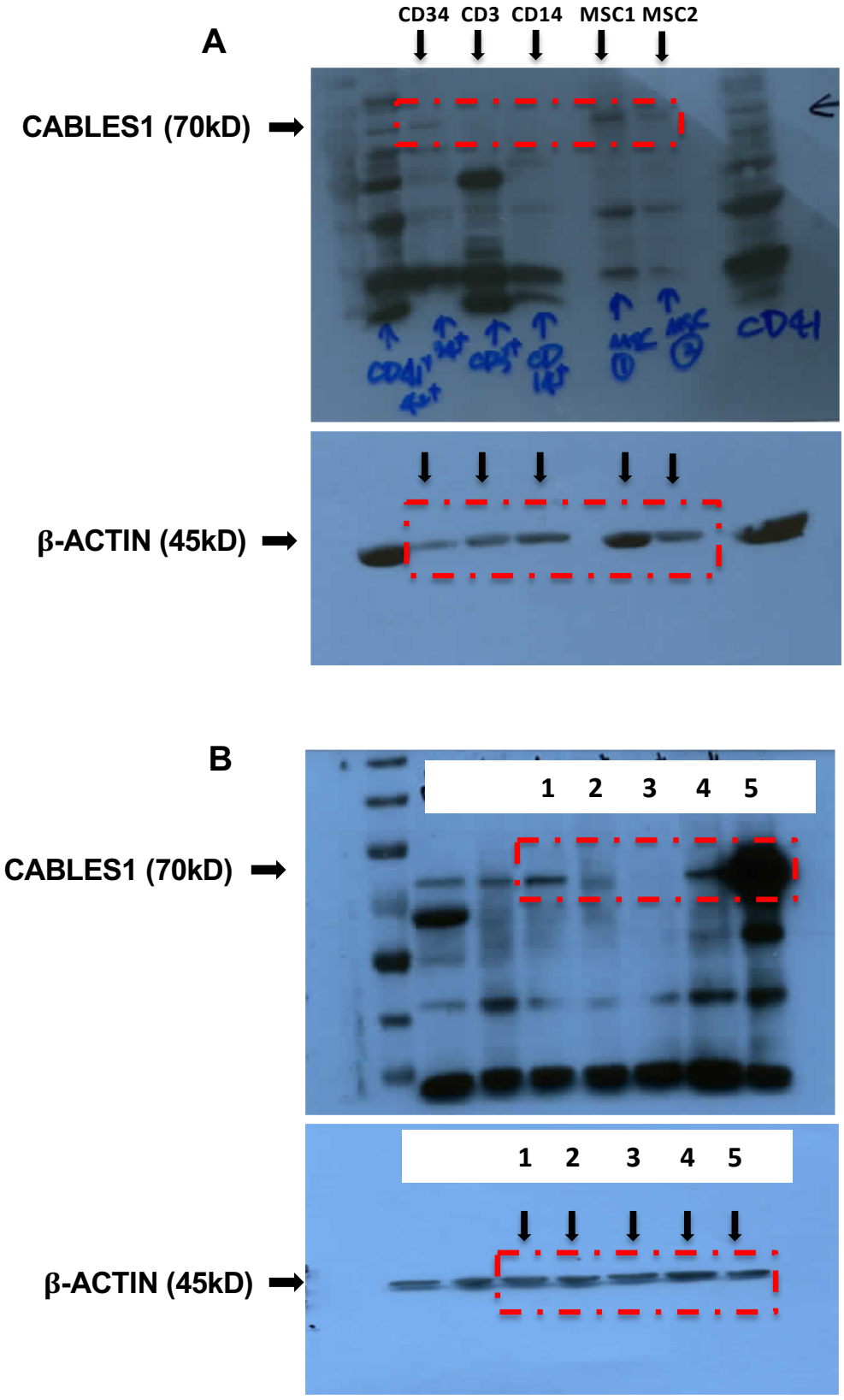

Figure S2. CABLES1 expression in hematopoietic and niche BM cells. (A) Uncropped Western blots with the indicated areas of selection shown in Figure 1C. Upper panel corresponds to CABLES1 and lower panel to **β**-ACTIN. **(B)** Uncropped blots for confirmation of CABLES1 antibody specificity using overexpression and shRNA mediated *Cables1* knockdown. 1: Scramble shRNA, 2: *Cables1* shRNA N1, 3: *Cables1* shRNA N2, 4: *GFP*-overexpressing, 5: CABLES1-GFP overexpressing cells. The signal corresponding to the expected 70kD band (corresponding to CABLES1 protein) was sharply diminished by shRNA treatment. Upper panel corresponds to CABLES1 and lower panel to **β**-ACTIN.

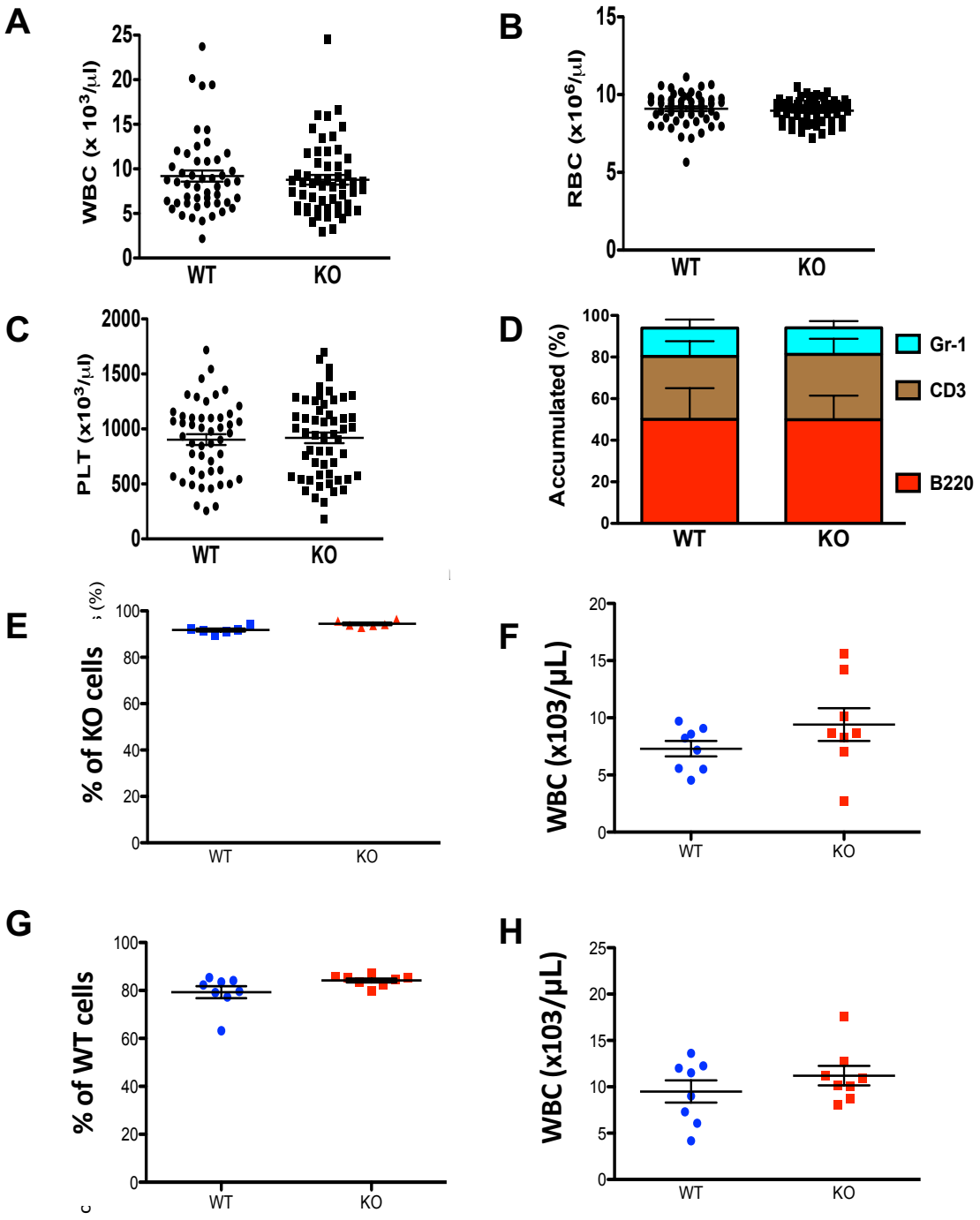

Figure S3: 10- to 12-week old *Cables1*$^{-/-}$ mice do not harbor obvious abnormalities in the hematopoietic compartment under steady state conditions. **(A)** WBC (white blood cells), **(B)** Red blood cells, **(C)** platelet (PLTs) counts, **(D)** percentages of B-lymphocytes, T-lymphocytes and myeloid cells within the peripheral blood in 5 mice per group. All values are expressed as mean ± SEM. **(E, F, G, H)** 5x10^6 BM cells from *Cables1* KO or WT mice were injected into *Cables1* WT or KO 9.5 Gy irradiated mice (n=8 per group). Percentage and white blood cells of KO (**E, F**) or WT (**G, H**) donor cells three months after injection. All values are expressed as mean ± SEM, no statistic differences were found using Student's unpaired two-tailed t-test.

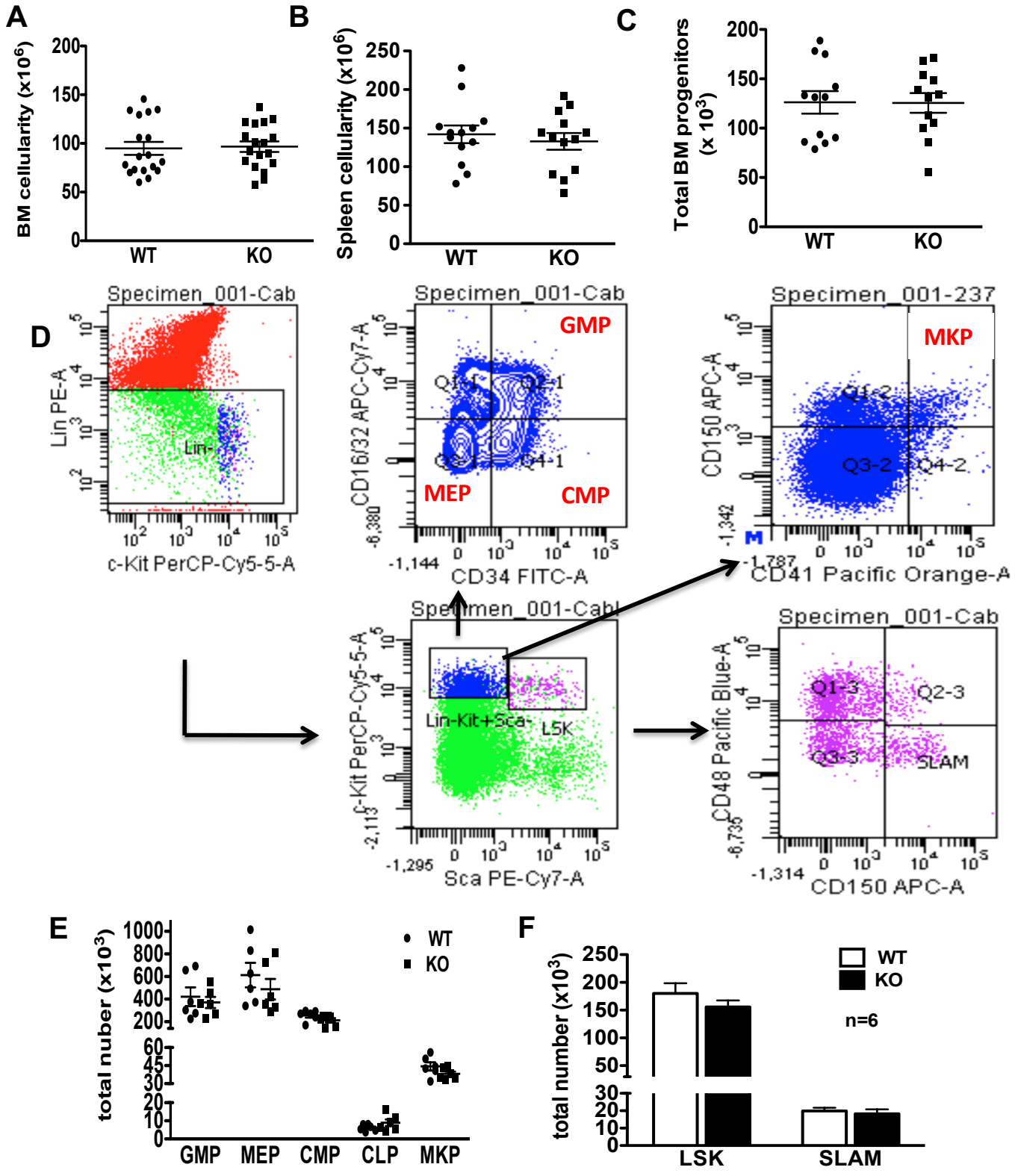

Figure S4: Analysis of HSPC within the BM in 10- to 12-week old *Cables1*$^{+/+}$ and *Cables1*$^{-/-}$ mice. (A) BM cellularity, **(B)** Spleen cellularity, **(C)** Total numbers of BM CFUs in *Cables1*$^{-/-}$ and *Cables1*$^{+/+}$ mice. **(D)** Full gating strategy with actual staining plots for immunophenotypic analysis of HSCs and progenitor cells. **(E)** Numbers of phenotypically defined GMP, CMP, CLP, MEP, MKP and **(F)** LSK and SLAM cells. GMP = granulomonocytic progenitors, CMP = common myeloid progenitors, CLP = common lymphoid progenitors, MEP = mega-erythroid progenitors, MKP = megakaryocytic progenitors. All values are expressed as mean ± SEM, no statistic differences were found using Student's unpaired two-tailed t-test.

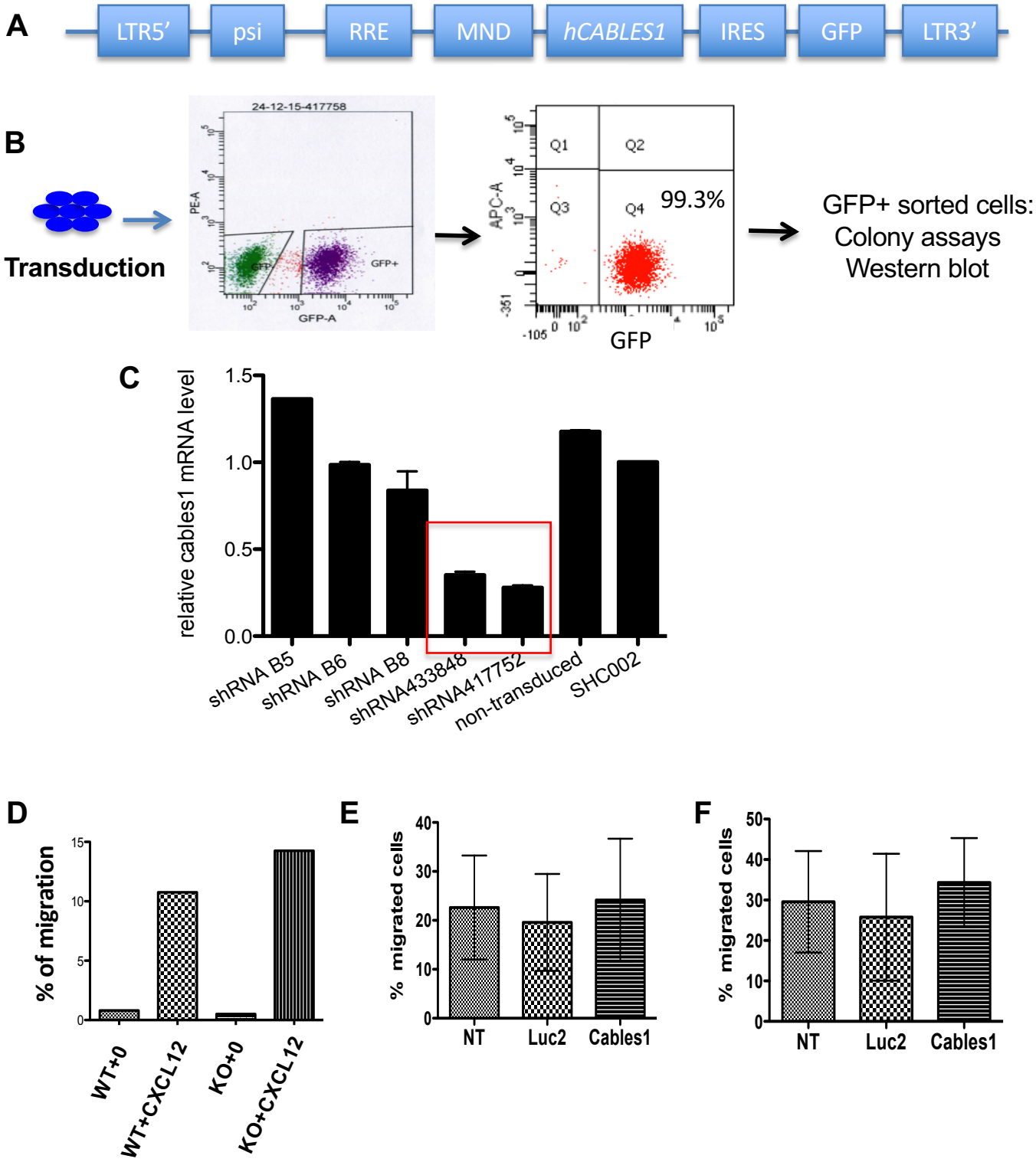

Figure S5: **Overexpression and shRNA strategy. (A)** pTrip lentiviral vectors encoding either GFP alone or human CABLES1 and GFP. **(B)** Prestimulated CB-CD34$^+$ cells were transduced and sorted on GFP expression for verification of CABLES1 expression. **(C)** *Cables1* mRNA expression was assessed by q-PCR after transduction of CD34+ cells with different human short hairpin RNAs (shRNAs) to *Cables1* or a control shRNA (shC002).**(D)** Chemotactic responses to CXCL12 of Lin$^-$ cells from BM *Cables1*$^{-/-}$ and littermate control mice (n=1). (**E**) Chemotactic responses to CXCL12 of HL-60 (n=3) and **(F)** U937 (n=3) cells either non transduced (NT) or transduced with lentiviral vectors encoding either GFP alone (Luc2) or human CABLES1 and GFP (Cables1). All values are expressed as mean ± SEM, statistic analysis was performed using Student's unpaired two-tailed t-test.

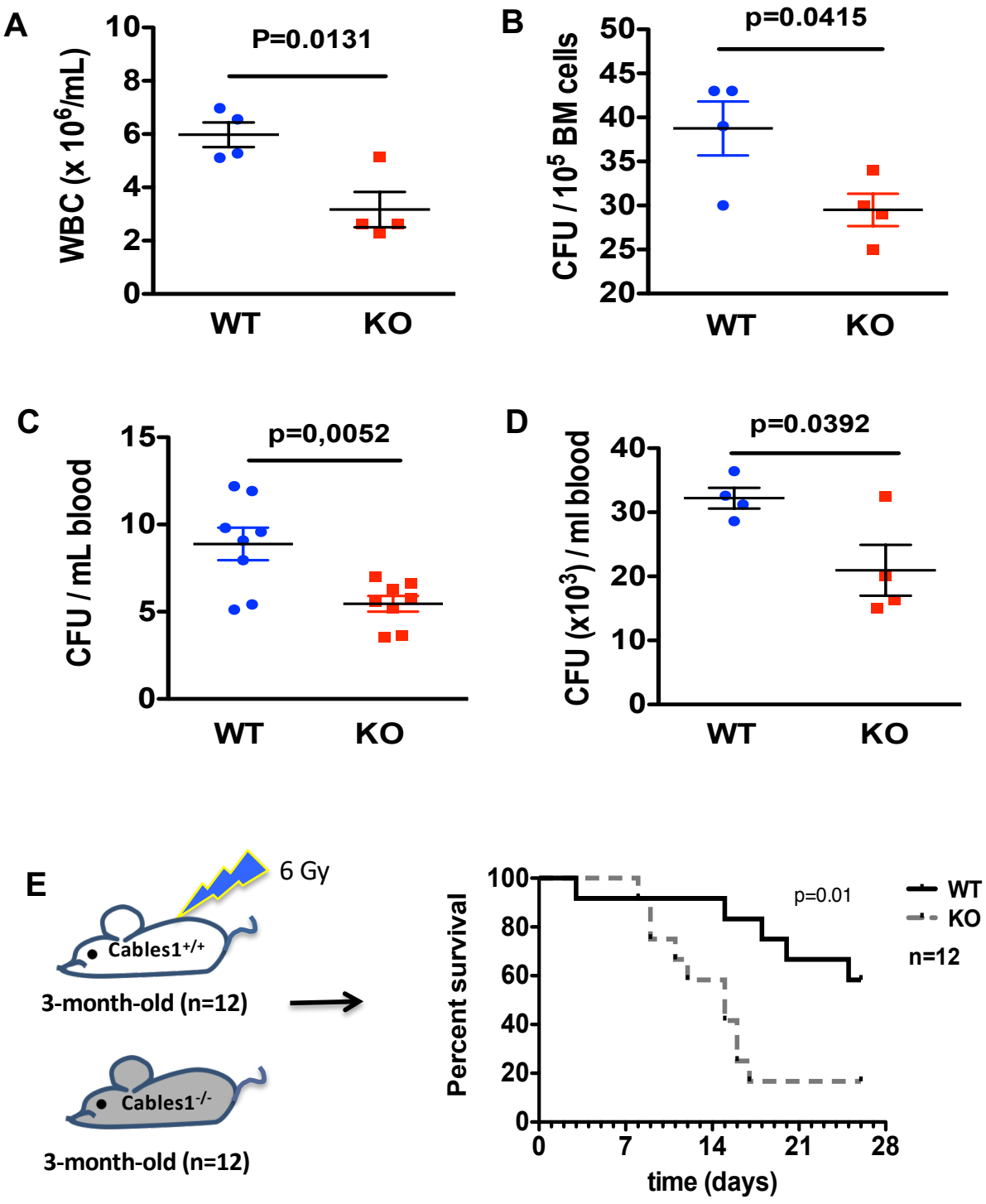

Figure S6 : **Impact of *Cables1* on hematopoietic regeneration and response to irradiation.** 3-month-old *Cables1*$^{-/-}$ and littermate control mice were injected intraperitoneally with 4 mg of CY followed by subcutaneous injection of 5 µg per day during 5 days of recombinant human G-CSF. **(A)** WBC, **(B)** BM CFU, **(C)** Blood CFU at day 4, **(D)** blood CFU at day 6. (**E)** 3-month-old *Cables1*$^{-/-}$ and littermate control mice were subjected to TBI (6 Gy) and survival was assessed (n=12). All values are expressed as mean ± SEM, statistic analysis was performed using Student's unpaired two-tailed t-test. Log-rank (Mantel-Cox) test was applied for comparing survival between WT and *Cables1*$^{-/-}$ mice.

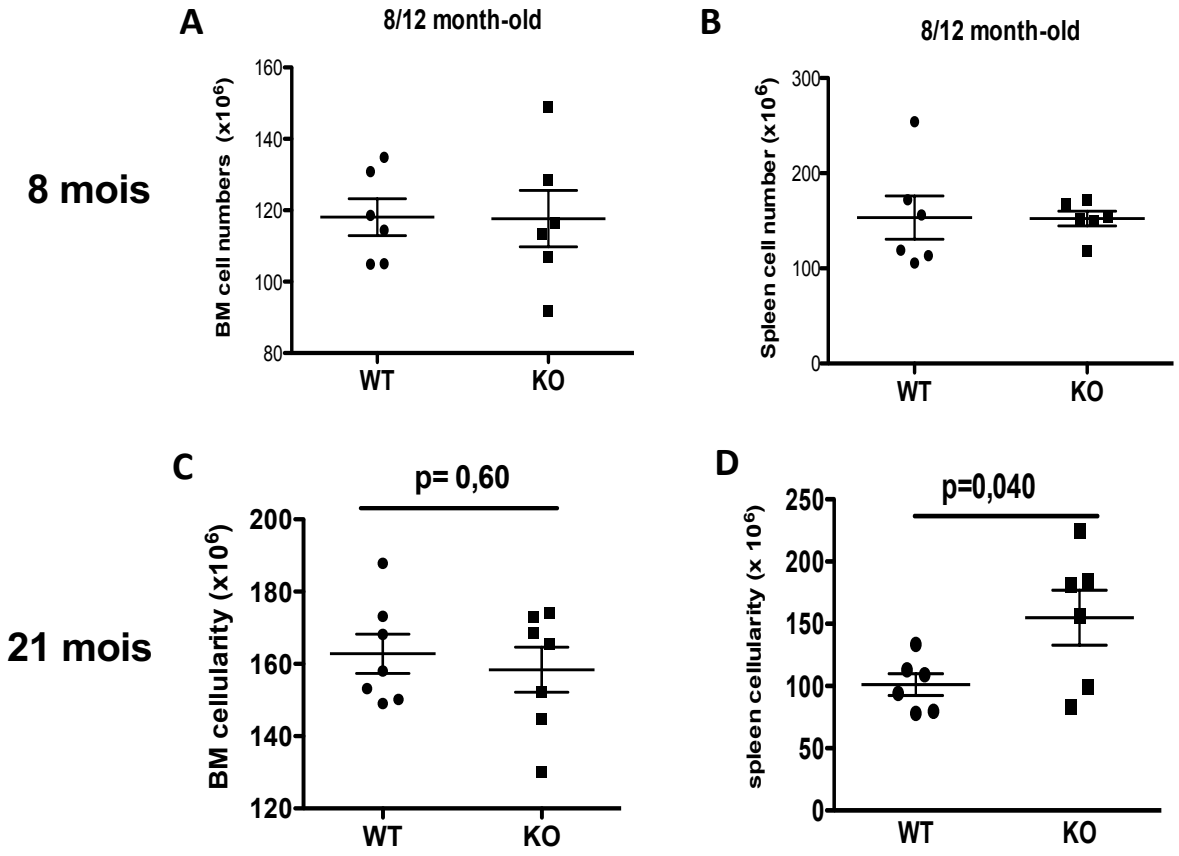

Figure S7: Bone marrow and spleen cellularities in WT and *Cables1* KO mice. (A) BM cellularity in middle-aged mice. **(B)** spleen cellularity in middle-aged mice. **(C)** BM cellularity in aged mice. **(D)** spleen cellularity in aged mice. All values are expressed as mean ± SEM, statistic analysis was performed using Student's unpaired two-tailed t-test.

Supplemental information

Murine bone marrow (BM) cell isolation

BM cells were extracted by centrifugation from intact hips, femora and tibiae, whereas spleens were gently mashed on a 70-μm nylon strainer to generate a single cell suspension. Cell collection was performed in PBS FCS 2% and filtered through a 70-μm nylon strainer. Nucleated cell numbers were measured on a Sysmex XP-300 counter (Sysmex, Lincolnshire, IL). All cell numbers were standardized as total count per two hips and legs, spleen, unless specified. Red blood cell lysis was performed using ACK buffer before staining. Cells harvested from tissues were immediately immunophenotyped.

Mouse BM progenitor cell analysis by flow cytometry

All staining analyses were performed on a BD FACSCanto™ II (BD Bioscience) flow cytometer. Hematopoietic progenitor cells were analyzed according to the following phenotypes: LSK cells ($Lin^-Kit^+Sca\text{-}1^+$), SLAM cells ($CD150^+CD48^-LSK$), granulomonocytic progenitors (GMP, $Lin^-Kit^+Sca\text{-}1^-CD34^+CD16^+/32^+$), common myeloid progenitors (CMP, $Lin^-Kit^+Sca\text{-}1^-CD34^+CD16^-/32^-$), mega-erythroid progenitors (MEP, $Lin^-Kit^+Sca\text{-}1^-CD34^-CD16^-/32^-$), common lymphoid progenitors (CLP, $Lin^-c\text{-}Kit^{int}Sca\text{-}1^{int}CD127^+CD135^+$) and megakaryocytic progenitors (MKP, $Lin^-Kit^+Sca\text{-}1^-CD41^+CD150^+$). Cells from the BM microenvironment were analyzed according to the following phenotypes: Mesenchymal stem cells (MSC, $CD45^-TER119^-CD31^-CD51^+Sca\text{-}1^+$), osteoblasts ($CD45^-TER119^-CD31^-CD51^+Sca\text{-}1^-$) and endothelial cells ($CD45^-TER119^-CD31^+$). The following mAbs were used: anti–mouse CD3 (clone 145-2C11, hamster IgG1), CD4 (clone RM4-5, rat IgG2a), CD (clone 53–6.7, rat IgG2a), CD11b (clone M1/70, rat IgG2b), CD16/32 (clone 93, rat IgG2a), CD34 (clone RAM34, rat IgG2a), CD41 (clone MWReg30, rat IgG1), CD45R/B220 (clone RA3-6B2, rat IgG2a), CD45.1 (clone A20, mouse IgG2a), CD45.2 (clone 104, mouse IgG2a), CD48 (clone HM48-1, Armenian hamster IgG), CD117 (clone 2B8, rat

IgG2b), CD127 (clone A7R34, rat IgG2a), CD135 (clone A2F10, rat IgG2a), CD150 (clone TC15-23F12,2, rat IgG2a), Ter119 (clone TER-119, rat IgG2b), Gr-1 (clone RB6-8C5, rat IgG2b), Sca-1 (clone E13-161,7, rat IgG2a). Antibodies were conjugated to biotin, BV 650, FITC, PE, APC, AF700, PE-cyanin (Cy) 5, PE-Cy7, eFluor 450, AF 647, APC-eFluor 780, peridinin chlorophyll protein PerCP-Cy5,5 or pacific blue and purchased from BD, eBioscience, or BioLegend. The lineage antibody cocktail included anti-CD3, anti-CD45R/B220, anti-CD11b, anti-TER119, and anti–Gr-1 mAbs. Secondary labeling was performed with Streptavidin–pacific orange from Thermo Fisher Scientific. Viability was assessed by adding 4′,6-diamidino-2-phenylindole (DAPI) at 0.5 μg/ml).

Fluorescence Activated Cell Sorting

For analyzing *Cables1* mRNA expression, 3-month-old wild type mice were used. Gr-1$^+$, B220$^+$, CD3$^+$, CD4$^+$ and CD8$^+$ cells were sorted from unfractionated BM or spleen, respectively. Progenitor cells were enriched using mouse hematopoietic progenitor (stem) cell enrichment set (Cat 558451; BD biosciences, USA) according to manufacturer's instructions. Depleted cells were then used for surface marker staining and sorted according to the phenotypes described above. For sorting niche component cells, femora, tibiae and hip bones were dissected and digested with collagenase I (Gibco) diluted with 1x Hanks' Balanced Salt Solution (HBSS; Gibco). Digested cells were stained with relevant antibodies according to the phenotypes described above. Cells were sorted by a BD FACSAria™ III cell sorter (BD bioscience, USA).

Immunofluorescence staining

100,000 freshly isolated CB CD34$^+$ cells were spun onto poly-lysine-coated slides. Cells were fixed with 2% paraformaldehyde/5% sucrose in PBS at room temperature (RT) for 15 min. Fixed cells were washed with PBS and permeabilized with 1% Brij in PBS for 2 min at RT. After

washing with PBS, cells were blocked for nonspecific binding sites with 1% bovine serum albumin and 1% defatted milk in PBS (BSA-milk-PBS). Then cells were incubated with mouse anti-CABLES1 (provided by Bo. R. Rueda) diluted in BSA-milk-PBS for 60 min at RT. They were then washed with PBS followed by incubation with FITC-conjugated anti-mouse secondary antibody for 30 min at RT (Molecular Probes). After washing 3 times with PBS, the slides were mounted with Vectorshield containing DAPI (Vector Labs, CA). Cells were examined under a Zeiss LSM 510 laser scanning fluorescence confocal microscope. To support the specificity of the staining, negative control for the immunostaining was done with T-lymphocytes.

In-vivo BrdU incorporation assay

Mice were injected i.p. with BrdU (1mg BrdU/g body weight) (Sigma) the first day. During the following 12 continuous days, mice were fed with BrdU-containing water (1mg/ml). BM cells were harvested, lineage depleted and cell surface was stained as described above. Cells were fixed and permeabilized with a BrdU staining kit (BD Biosciences). Samples were incubated with DNAse I for one hour at 37°C, followed by intra-cellular staining with anti-BrdU-FITC (Cat. 557891 FITC BrdU Flow Kit BD Pharmingen San Diego, CA). Cells were washed and suspended in Permwash buffer containing 10 μg/ml DAPI. Samples were analyzed by flow cytometry (BD FACSCanto™ II, BD Bioscience, USA).

Assessment of colony-forming cell (CFC) potential

To assess the clonogenic potential, BM mononucleated cells (BMMNCs) were plated at a density of 50,000 cells per ml methylcellulose medium, spleen cells were plated at a density of 100,000 cells per ml methylcellulose medium. Whole PB (25 μl blood per plate) was lysed with Ammonium-Chloride-Potassium (ACK) solution to eliminate red blood cells. After two washes with PBS containing 5% FBS (PBS-5% FBS), lysed cells were plated in methylcellulose medium

(MethoCult™ M3234, STEMCELL Technologies) (Foudi et al., 2006). The cultures were maintained at 37°C in a humidified atmosphere containing 5% CO_2. Colonies derived from colony forming cells (CFC) were scored at day 7-12 under an inverted microscope (Nikon, Japan).

Homing experiments

BM cells (15 $\times 10^6$/host) from *Cables1*$^{+/+}$ or *Cables1*$^{-/-}$ mice (3 month-old) were stained with the cell tracker carboxyfluorescein-succinimidyl ester (CFSE), and marked cells were injected through the retro-orbital vein into previously irradiated (9.5 Gy) mice (Foudi et al., 2006). Four or 16 hours after injection, mice were sacrificed, PB was collected and one femur and the spleen were dissected for analysis. The numbers of CFSE$^+$ cells in PB, BM and spleen were detected by flow cytometry.

Separation of cells in the G0/G1/SG2M phase by Hoechst and Pyronin Y staining

BM cells from wild type mice were used for sorting of LSK cells in the G0, G1 and S/G2/M phase. To this end unfractionated BM cells were depleted and stained for LSK phenotype. Stained cells were then incubated with 10 μg/ml Hoechst 33342 (Sigma Chemical Co, St Louis, MO) for 1.5 hours at 37°C in Hanks balanced salt solution (HBSS) medium, supplemented with 2mM Hepes, 10% FBS and 1mg/l glucose. During the last 45 min of incubation, cells were co-incubated with 0.5 μg/ml Pyronin Y (RNA dye) (Sigma Chemical Co, St Louis, MO). G0, G1 and S/G2/M phase LSK cells were sorted by BD FACSARIA III device.

Chemotactic assays

Chemotaxis assays were performed as previously described (Riviere et al., 1999). Briefly, Lin- cells (10^5) or transduced cells (Hl-60 or U937 cells) were added to the upper chambers of a 24-well plate with 5-μm-pore-size Transwell inserts (EMD Millipore), containing or not 100 ng/ml of

CXCL12 (Peprotech, France) in the lower chamber. Lin- migrated cells were enumerated by CFU-C mix assay after 4 hours of incubation at 37°C, 5% CO_2 and referred to input BM CFU-Cs to obtain a migration percentage.

Western blot

Separated cells were lysed in 2x Laemmli buffer and Protease Inhibitor Cocktail (company). Protein lysates were separated on 10% SDS-PAGE 100 V for 3 hours. Proteins were transferred onto polyvinylidene difluoride (PVDF) membrane by wet electroblotting. The membrane was blocked in blocking buffer for one hour and incubated with primary antibody overnight. PVDF membrane was washed with TBST, then incubated with secondary antibody. Membrane was washed with TBST for 50 min, incubated with chemiluminescence substrate for oner min and exposed to Kodak autoradiography film.

RNA extraction and quantitative polymerase chain reaction (qPCR)

Total RNAs were prepared using **Direct-zol™ RNA Kit** (Zymo Research Corp., Irvine, USA). First-strand cDNA was synthesized by using the SuperScript II Reverse Transcriptase (Life Technologies, Carlsbad, USA). PCR reactions were carried out in the ABI Prism GeneAmp 5700 Sequence Detection System using Takyon SYBR MasterMix (Eurogentec, France). The expression levels of *Cables1* were calculated relatively to the expression of HPRT and SDHA as endogenous housekeeping controls. Mouse brain and $CD34^+$ cells were used as reference for *Cables1* expression level in murine and human cells, respectively. Primer sequences are listed in Table1.

Table 1 : primers used in this study

Mouse *Cables1*	F	CCT-TCA-TAC-ATG-ACC-ACA-GTG-A
	R	TCA-GGC-TCC-TGA-TTT-TGC-T
Mouse *Hprt*	F	TGA-TTA-TGG-ACA-GGA-CTG-AAA-GA
	R	AGC-AGG-TCA-GCA-AAG-AAC-TTA-TAG
Mouse *Sdha*	F	AAG-TTG-AGA-TTT-GCC-GAT-GG
	R	TGG-TTC-TGC-ATC-GAC-TTC-TG
Mouse *Zfy1*	F	TGG-AGA-GCC-ACA-AGC-TAA-CCA
	R	CCC-AGC-ATG-AGA-AAG-ATT-CTT
Mouse *Bcl2*	F	AAG-CTG-TCA-CAG-AGG-GGC-TA
	R	CAG-GCT-GGA-AGG-AGA-AGA-TG
Human *CABLES1*	F	CCT-TGG-AGA-CCC-TGG-AAG-AT
	R	GCC-ATT-CCT-GGT-ATC-GTG-TT
Human *MRPL32*	F	CTG-CAG-TCT-CCT-TGC-ACA-CCT
	R	TGT-CCT-GAA-TGT-GGT-CAC-CTG-A
Human *SDHA*	F	TGG-TTG-TCT-TTG-GTC-GGG
	R	GCG-TTT-GGT-TTA-ATT-GGA-GGG